Molecular Pharmacology Fast Forward. Published on March 9, 2010 as doi: 10.1124/mol.109.062018
This article has not been copyedited and formatted. The final version may differ from this version.

MOL 62018

PAR1 and PAR2 couple to overlapping and distinct sets of G proteins and linked signaling pathways to differentially regulate cell physiology

Kelly L. McCoy, Stephen F. Traynelis, and John R. Hepler*

Department of Pharmacology, Rollins Research Center, Emory University School of Medicine, G205 Rollins Research Center, 1510 Clifton Road, Atlanta, GA 30322, USA

Molecular Pharmacology Fast Forward. Published on March 9, 2010 as DOI: 10.1124/mol.109.062018
This article has not been copyedited and formatted. The final version may differ from this version.

Running Title Page

Running title: Differential coupling of PAR1 and PAR2 to G protein pathways

Number of text pages: 25 (excluding figure legends)

Number of figures: 8

Number of references: 45

Number of words in abstract: 249

Number of words in introduction: 557

Number of words in discussion: 1,470

List of non-standard abbreviations: BBB, blood-brain barrier; BSA, bovine serum albumin; CNS, central nervous system; DMEM, Dulbecco's modified Eagle medium; ECL, enhanced chemiluminescence; ERK, extracellular signal-regulated kinase; GPCR, G protein-coupled receptor; GRK2, G protein-coupled receptor kinase-2; InsPs, inositol phosphates; MAPK, mitogen activated protein kinase; PAR, protease-activated receptor; PAR-APs, PAR-activating peptides; PBS, phosphate-buffered saline; PLC, phospholipase C; PTX, pertussis toxin; RGS, regulator of G protein signaling; TBST, Tris-buffered saline

*Corresponding Author:

John R. Hepler, Ph.D.
1510 Clifton Road
G205 Rollins Research Center
Atlanta, GA 30322
Email: jhepler@emory.edu
Telephone: +1 404 727 8192
Fax: +1 404 727 0365

Molecular Pharmacology Fast Forward. Published on March 9, 2010 as DOI: 10.1124/mol.109.062018
This article has not been copyedited and formatted. The final version may differ from this version.

Abstract

The protease-activated receptors (PAR1 and PAR2) are unusual G protein-coupled receptors that are activated by distinct serine proteases and are co-expressed in many different cell types. Limited recent evidence suggests these closely related receptors regulate different physiological outputs in the same cell, though little is known about the comparative signaling pathways utilized by these receptors. Here we report that PAR1 and PAR2 couple to overlapping and distinct sets of G proteins to regulate receptor-specific signaling pathways involved in cell migration. In functionally PAR-null COS-7 cells, ectopically expressed PAR1 and PAR2 both form stable complexes with $G\alpha_q$, $G\alpha_{11}$, $G\alpha_{14}$, $G\alpha_{12}$ and $G\alpha_{13}$. Surprisingly, PAR1 but not PAR2 coupled to $G\alpha_o$, $G\alpha_{i1}$ and $G\alpha_{i2}$. Consistent with these observations, PAR1 and PAR2 stimulation of inositol phosphate production and RhoA activation was blocked by specific inhibitors of $G_{q/11}$ and $G_{12/13}$ signaling, respectively. Both receptors stimulated ERK1/2 phosphorylation, but only PAR1 inhibited adenylyl cyclase activity, and pertussis toxin blocked PAR1 effects on both adenylyl cyclase and ERK1/2 signaling. Neu7 astrocytes express native PAR1 and PAR2 receptors that activate inositol phosphate, RhoA, and ERK1/2 signaling. However, only PAR1 inhibited adenylyl cyclase activity. PAR1 and PAR2 also stimulate Neu7 cell migration. PAR1 effects on ERK1/2 phosphorylation and cell migration were blocked both by pertussis toxin and by the MEK/ERK inhibitor (U0126), whereas PAR2 effects were only blocked by U0126. These studies demonstrate that PAR1 and PAR2 physically and functionally link to overlapping and distinct profiles of G proteins to differentially regulate downstream signaling pathways and cell physiology.

Molecular Pharmacology Fast Forward. Published on March 9, 2010 as DOI: 10.1124/mol.109.062018
This article has not been copyedited and formatted. The final version may differ from this version.

Protease-activated receptors (PARs) are a family of four G protein-coupled receptors (GPCRs) that are irreversibly activated through proteolytic cleavage of their N-termini by serine proteases (e.g., thrombin, trypsin, plasmin and others). This cleavage creates new extracellular N-termini, which serve as tethered ligands that intramolecularly activate the receptors and initiate complex intracellular signaling events (Macfarlane et al., 2001;Traynelis and Trejo, 2007). PAR1 was first discovered as a receptor for thrombin (Vu et al., 1991). As such, it is best known for its role in the cardiovascular system's coagulation cascade and hemostatic mechanisms (Coughlin, 2005). A broader understanding of PAR1 and the cloning of three additional PARs (PAR2-4) (Nystedt et al., 1994;Ishihara et al., 1997;Xu et al., 1998) has implicated them in strikingly diverse pathophysiological functions including stroke, inflammation, reactive gliosis, and cancer (Ossovskaya and Bunnett, 2004).

With regard to the role of PARs in stroke, mounting evidence implicates PAR1 and PAR2 in reactive gliosis following head injury and/or hemorrhagic stroke, which lead to the breakdown of the blood-brain barrier (BBB) of the central nervous system (CNS) (Traynelis and Trejo, 2007) (and references therein). Since PARs are expressed in both glia and neurons, as well as in many other cells (Macfarlane et al., 2001;Ossovskaya and Bunnett, 2004), this leakage of serine proteases into the CNS provides PAR activators with direct access to their receptors following stroke and ischemia. PARs are thought to influence astrogliosis, which contributes to glial scarring and to the subsequent rebuilding of the BBB (Nicole et al., 2005;Nishino et al., 1993;Pindon et al., 2000). Conflicting reports have implicated PAR1 specifically in both neurodegeneration and neuroprotection, depending on the concentration of the activating protease (Hamill et al., 2009;Traynelis and Trejo, 2007) (and references therein). Whether these effects are more beneficial or harmful to recovering brain tissue remains unresolved. Furthermore, the molecular details underlying the function of PARs in these cells are not fully elucidated.

Molecular Pharmacology Fast Forward. Published on March 9, 2010 as DOI: 10.1124/mol.109.062018
This article has not been copyedited and formatted. The final version may differ from this version.

PAR1 and PAR2 often are expressed in the same cells. In mediating their physiological effects, these closely related receptors have been reported to activate multiple G protein-linked signaling pathways including mitogen-activated protein kinase (MAPK), phospholipase C (PLC), and intracellular calcium (Macfarlane et al., 2001;Traynelis and Trejo, 2007;Dery et al., 1998). PAR1 appears to functionally couple to one or more of the $G_{q/11}$, $G_{i/o}$, and $G_{12/13}$ subfamilies (Macfarlane et al., 2001;Traynelis and Trejo, 2007), and a previous screen for direct PAR1 binding partners found that G_{i2} and $G_{q/11}$ both co-immunoprecipitate (co-IP) with PAR1 in human neuroblastoma cells (Ogino et al., 1996). Several studies also have suggested that activating PAR2 triggers responses traditionally mediated by $G_{q/11}$, $G_{i/o}$ and $G_{12/13}$ (Macfarlane et al., 2001;Traynelis and Trejo, 2007). However, a comprehensive understanding of the G protein signaling pathways stimulated by PAR1 and PAR2 in the same cell is lacking.

In the present study, we sought to define the G protein coupling and signaling profiles of PAR1 and PAR2 in the same cellular context and to identify differences in their physiological roles. Using both ectopic cellular systems expressing recombinant proteins (COS-7 kidney cells lacking functional PAR readouts) and cells of neuronal origin that natively express PARs (Neu7 astroglia), we have found that PAR1 and PAR2 couple to overlapping and distinct sets of G proteins and linked signaling pathways to modulate different cellular responses. In doing so, we have highlighted previously unappreciated differences between these two closely related receptors.

Molecular Pharmacology Fast Forward. Published on March 9, 2010 as DOI: 10.1124/mol.109.062018
This article has not been copyedited and formatted. The final version may differ from this version.

Materials and Methods

Materials were obtained from the following sources: Anti-FLAG M2 affinity gel and anti-FLAG M2 monoclonal antibody-peroxidase conjugate, bovine serum albumin (BSA), isoproterenol, U73122, L-(-)-Norepinephrine, penicillin, and streptomycin from Sigma Chemical Co. (St. Louis, MO); fetal bovine serum from Atlanta Biologicals (Atlanta, GA); trypsin, Dulbecco's modified Eagle's medium (DMEM) from Cellgro (Herndon, VA); Lipofectamine 2000 transfection reagent from Invitrogen (Carlsbad, CA); *myo*-[^{3}H]inositol from American Radiolabeled Chemicals, Inc.(St. Louis, MO); RhoA G-LISA™ Activation Assay colorimetric format kit and C3 exoenzyme from Cytoskeleton, Inc. (Denver, CO); cAMP ELISA Kit (colorimetric) from Cell Biolabs, Inc. (San Diego, CA); conjugated goat anti-mouse monoclonal antibody from Rockland Inc. (Gilbertsville, PA); Pertussis toxin (PTX) was purchased from List Biologicals (Campbell, CA); p44/42 ERK1/2 (extracellular signal-regulated kinase 1/2) antibody, phospho-p44/42 ERK1/2 antibody, MEK1/2 inhibitor U0126, and bisindolymaleimide (BIS) from Cell Signaling Technology (Beverly, MA); Glu-Glu monoclonal antibody (anti-EE) from Covance, Inc. (Princeton, NJ), anti-$G\alpha_s$, anti-$G\alpha_o$ anti-$G\alpha_{i1}$, anti-$G\alpha_{i2}$, anti-$G\alpha_{i3}$, anti-$G\alpha_{12}$, and anti-$G\alpha_{13}$ antibodies from Santa Cruz Biotechnology, Inc. (Santa Cruz, CA); anti-$G\alpha_q/_{11}/_{14}$ antibody Z811 was kindly provided by Dr. Paul Sternweis (U. Texas Southwestern, Dallas, TX); peroxidase-conjugated goat anti-mouse IgG antisera from Rockland Immunochemicals, Inc. (Gilbertsville, PA), and peroxidase-conjugated goat anti-rabbit was from Bio-Rad (Hercules, CA). The PAR-activating peptides (PAR-APs), TFLLR-NH_2 (TFLLR) and 2-furoyl-LIGRLO-NH_2 (LIGRLO), were synthesized by Dr. Jan Pohl at the Emory University Microchemical Facility (Atlanta, GA).

cDNA constructs

Molecular Pharmacology Fast Forward. Published on March 9, 2010 as DOI: 10.1124/mol.109.062018
This article has not been copyedited and formatted. The final version may differ from this version.

PAR1 and PAR2 constructs: Mouse PAR1-FLAG and PAR2 are both in the pcDNA3.1 vector. A C-terminal FLAG epitope tag was added to PAR2 by PCR amplification of BamHI-XhoI fragment that contained the FLAG sequence. An antisense primer was designed to eliminate the stop codon of the PAR2 sequence and introduce the FLAG sequence with a new C-terminal stop codon. The antisense primer was 5'-CTCGAGTTACTTGTCATCGTCGTCCTTGTAGTCGTAGGAGGTTTTAACAC-3' and was used in combination with either the sense primer 5'-CGGGGATCCATGCGAAGTCTCAGCCTGGCG-3' to generate a BamHI-XhoI fragment from the existing pcDNA3.1 sequence.

RGS protein constructs: p115-RGS and GRK2-RGS, truncated RGS proteins used as selective G protein pathway inhibitors, were kindly provided by Dr. T. Kendall Harden (UNC-Chapel Hill, Chapel Hill, NC) and were created as previously described (Hains et al., 2004).

Cell culture and transfections – COS-7 (ATCC® Number CRL-1651™) and Neu7 (a generous gift from Dr. Isobel Scarisbrick, Rochester, MN) cells were propagated in DMEM with sodium pyruvate supplemented with 10% heat inactivated fetal bovine serum, 100 μg/mL streptomycin and 100U/mL penicillin at 37°C in a humidified atmosphere with 5% CO_2. Subculturing of confluent plates was done at a ratio of 1:10 for transfection. COS-7 cells were transfected according to Lipofectamine 2000® transfection reagent protocol and cells were used for experimentation 24-48 h after transfection.

Immunoblot Analysis—Nitrocellulose membranes were blocked in blocking buffer (50 mM Tris, pH 7.4, 150 mM NaCl, 5% milk, 0.5% Tween 20, 0.02% sodium azide) at room temperature for 1 h and subsequently incubated in a primary antibody dilution for 3 h at room temperature or overnight at 4°C. Dilutions differed for each antibody and are listed here: anti-FLAG 1:1000,

Molecular Pharmacology Fast Forward. Published on March 9, 2010 as DOI: 10.1124/mol.109.062018
This article has not been copyedited and formatted. The final version may differ from this version.

anti-p44/42 ERK1/2 1:300 and anti-phospho p44/42 1:1000 in Tris-buffered saline + 0.1% Tween 20 (TBST) with 5% BSA; anti-$G\alpha_q$ family Z811 1:2000, anti-$G\alpha_o$ 1:200, anti-$G\alpha_{i1}$ 1:150; anti-$G\alpha_{i2}$ 1:150; anti-$G\alpha_{i3}$ 1:150; anti-$G\alpha_{12}$ 1:200; anti-$G\alpha_{13}$ 1:200, and anti-Gβ 1:150 in blocking buffer. Membranes were washed three times with TBST and then probed with horseradish peroxidase-conjugated secondary antisera for 1 h at room temperature. For secondary antibodies the dilutions were: goat anti-rabbit IgG 1:25,000 in TBST and goat anti-mouse IgG 1:20,000 in TBST. The protein bands were visualized using enhanced chemiluminescence (ECL) and exposed to film.

Measurement of [^{3}H]InsP formation – Levels of [^{3}H]inositol phosphates ([^{3}H]InsPs) accumulation were determined in confluent 12-well plates. Untransfected Neu7 cells or COS-7 cells transiently transfected with PARs alone or in combination with either the $G_{q/11}$-pathway inhibitor GRK2-RGS, or the $G_{12/13}$ pathway inhibitor p115-RGS were metabolically labeled with *myo*-[^{3}H]inositol in serum-free media for 18-24 h. Due to difficulty transfecting Neu7 cells, pharmacological inhibitors of PLC signaling (U73122) or Rho signaling (C3 toxin) were added during the last 30 min or 4 h of serum starvation, respectively. After pre-labeling, medium containing *myo*-[^{3}H]inositol was removed and incubation buffer (DMEM buffered with 25mM HEPES, pH 8.0, and containing 10 mM $LiCl_2$) was added to each well for 20 min. Cells were incubated with PAR-APs for 5 min. Cells were then solubilized with 20 mM formic acid, neutralized with 0.7 M NH_4OH, and centrifuged for 5 min at 10,000 x g at 4^{o}C. [^{3}H]InsPs were separated by anion exchange chromatography (AG 1-X8 Dowex, Bio-Rad) using increasing amounts of ammonium formate. Samples were subjected to anion exchange chromatography to isolate [^{3}H]InsPs, which were quantified by scintillation counting and expressed as mean ± S.E.M.

Molecular Pharmacology Fast Forward. Published on March 9, 2010 as DOI: 10.1124/mol.109.062018
This article has not been copyedited and formatted. The final version may differ from this version.

Two-electrode voltage clamp recordings from Xenopus laevis oocytes: Oocytes were harvested from *Xenopus laevis (X. laevis)* were defolliculated and maintained in 1x Barth's culture solution at 16ºC. Stage V-VI oocytes were either injected with 5ng PAR1 or PAR2 cRNA, which was synthesized from cDNA according to the manufacturer's specifications (Ambion, TX). Recordings were performed 4-5 days after injections. The recording solution contained (in mM) 60 NaCl, 38 KCl, 2.3 $CaCl_2$, 1 $MgCl_2$, and 6 HEPES. The pH was adjusted to 7.4 with NaOH. Patch pipettes with tip diameters of 1-2 µm were used as electrodes and filled with 300 mM KCl. Current responses were recorded at a holding potential of -40 mV. Data was acquired and voltage was controlled with a two-electrode voltage-clamp amplifier (OC-725; Warner Instruments, Hamden, CT). The PAR-APs diluted in 1x Barth's to final concentrations of 30µM TFLLR and 10µM LIGRLO, respectively, were used to elicit the $I_{Cl(Ca)}$.

Measurement of ERK1/2 phosphorylation: After serum starvation in the absence or presence of pharmacological inhibitors (PTX overnight, C3 toxin for 4 hours, U73122 for 30 minutes, and BIS for 30 minutes), untransfected Neu7 cells or COS-7 cells separately transfected with PAR1 or PAR2 were stimulated with the PAR-APs for 2-5 min, harvested, sonicated, boiled in sample buffer, subjected to SDS-polyacrylamide gel electrophoresis (SDS-PAGE; 13.5%) and transferred to nitrocellulose membranes. Membranes were blocked and washed once in TBST + 5% BSA followed by overnight incubation with p44/42 ERK1/2 and phospho- p44/42 ERK1/2 antibodies at 4ºC. Membranes were washed with TBST and incubated for 1 h with HRP-conjugated goat anti-rabbit IgG. The membranes were again washed and protein bands were detected by ECL. Densitometry was performed using Image J software (NIH website), and samples were normalized by dividing phospho-ERK densitometry units by total ERK Densitometry units and expressing these numbers as a percent of maximal ERK phosphorylation. Two-way ANOVA analyses were performed using SigmaStat software (Aspire Software International; Ashburn, VA).

Molecular Pharmacology Fast Forward. Published on March 9, 2010 as DOI: 10.1124/mol.109.062018
This article has not been copyedited and formatted. The final version may differ from this version.

Measurement of RhoA activation: The GTP-bound form of RhoA was measured using the absorbance-based RhoA Activation G-LISA™ kit (Cytoskeleton, Inc., Denver, CO) according to the manufacturer's protocol. Before using the kit's components, Neu7 cells or transiently transfected COS-7 cells were serum-starved overnight and then treated for 2 min with the PAR-APs in the presence or absence of the rho inhibitor, C3 toxin or the transfected G_{12}-pathway inhibitor, p115-RGS. The absorbance from the G-LISA™ plate was read by a spectrophotometer at a wavelength of 490nm.

Co-Immunoprecipitation of PAR/G protein complexes—COS-7 cells were transfected in 15 cm plates with a total of 40µg of DNA per plate (20µg of receptor + 20µg G protein; empty vector was used in place of either component, receptor or G protein, for the controls) for 18-24 h. The following day, cells were washed in PBS and harvested in 0.5 mL of Tris Buffer (50mM Tris, pH 7.4, 5 mM $MgCl_2$, 1 mM EGTA, 150 mM NaCl, 1 mM EDTA, and a protease inhibitor pellet), and sonicated. In experiments with agonist, PAR-APs or norepinephrine were added to lysates for 30 min. *n*-Dodecyl-β-D-maltoside (DβM; Calbiochem) was added to a final concentration of 2%. Membrane proteins were extracted with 2% DβM for 3 h, rotating end-over-end at 4°C, and debris was pelleted by ultracentrifugation (100,000 x *g*, 4°C, 30 min). An aliquot of the lysate was kept to be run as "input" on gel. Remaining cytosol was incubated overnight at 4°C with anti-FLAG M2 affinity gel, rotating end-over-end. The following day, the anti-FLAG resin was pelleted and washed three times with Tris Buffer containing 0.2% DβM. The resin then was resuspended in 2X Laemmli Sample Buffer (100mM Tris, pH 6.8, 0.5% SDS, 20% glycerol, 0.5% β-mercaptoethanol, 0.004% bromophenol blue). Following recovery by centrifugation, entire supernatants were loaded onto 11% polyacrylamide gels for SDS-PAGE separation. Samples for immunoblot analysis were transferred to nitrocellulose membranes, and immunoblotting was carried out as described.

Molecular Pharmacology Fast Forward. Published on March 9, 2010 as DOI: 10.1124/mol.109.062018
This article has not been copyedited and formatted. The final version may differ from this version.

Measurement of cAMP inhibition: cAMP inhibition was measured using the absorbance-based cAMP ELISA kit (Cell Biolabs, Inc., San Diego, CA) according to the manufacturer's protocol. Before using the kit's components, transiently transfected 12-well plates of COS-7 or untransfected Neu7 cells were plated overnight and then treated for 2 min with isoproterenol, PAR-APs, and the phosphodiesterase inhibitor IBMX in the presence or absence of PTX. The absorbance from the ELISA plate was read by a spectrophotometer at a wavelength of 450nm.

Wound-scratch test to measure migration: Migration of Neu7 cells was measured using a wound-scratch test. Briefly, cells were grown to confluence in 6-well plates and the cell monolayer was "wounded" by using a 0.5-10µL pipette tip to scratch a line across the monolayer. Immediately after wounding, cell media was replaced with serum-free media containing vehicle, 100µM TFLLR, or 200µM LIGRLO in the presence or absence of 100 ng/mL PTX or 10µM U0126. Pictures were taken with an Olympus IX51 light microscope at time 0 and 24 h after agonist addition. Quantification of the cell migration images was achieved using ImageJ software (NIH website). The total area of the "wound" was highlighted and quantified and cell migration was determined by subtracting the cell-free area from the total area covered by cells (expressed as a percent of total area of the wound). Statistical *T* tests were performed on figures obtained from analyzing two different images for each condition. Graphpad Software (Graphpad Software, Inc.) was used to perform statistical analysis.

Measurement of [^{3}H] Thymidine Incorporation: Proliferation of Neu-7 cells was measured as previously described (Sorensen et al., 2003). Briefly, cells were plated and serum starved for 24 h in the absence or presence of PTX. Cells were then challenged with agonist (vehicle, TFLLR or LIGRLO) for 24 h. During the final 2 h of stimulation, [^{3}H]thymidine was added to a final concentration of 1 µCi/mL. Cells were washed in ice-cold PBS and then 20% trichloroacetic acid

Molecular Pharmacology Fast Forward. Published on March 9, 2010 as DOI: 10.1124/mol.109.062018
This article has not been copyedited and formatted. The final version may differ from this version.

was added for 30 min at 4°C. Cells were again washed in PBS, and the acid-insoluble material was lysed in 0.1 N NaOH/1% SDS. [^{3}H]Thymidine in lysates was measured by scintillation counting.

Molecular Pharmacology Fast Forward. Published on March 9, 2010 as DOI: 10.1124/mol.109.062018
This article has not been copyedited and formatted. The final version may differ from this version.

Results

PAR1 and PAR2 link to multiple G protein-regulated pathways— PAR1 and PAR2 have both been reported to activate signaling pathways regulated by $G_{q/11}$, $G_{i/o}$, and $G_{12/13}$. To define which signaling pathways PAR1 and PAR2 are linked to in a defined biological system, we screened various cell lines to identify a model system that did not respond to either of the specific PAR-activating proteins (PAR-APs; i.e., TFLLR for PAR1 or LIGRLO for PAR2). Previous studies have reported that COS-7 cells express undetectable (or very low) levels of PARs (Blackhart et al., 2000;Ishihara et al., 1997), and showed that COS-7 cells do not activate inositol phosphate or calcium signaling in response to stimulation with TFLLR, thrombin, trypsin, or other proteases. Consistent with these reports, we found that our COS-7 cells did not respond to either peptide in various signaling assays (as shown in basal and vector controls, Figs. 1, 4C-D, 5) and that these cells could be readily transfected to express recombinant receptors and G proteins. Over many repeated experiments, we found that both PAR1 and PAR2 proteins consistently express well when transfected into in COS-7 cells (Supplemental Fig. S1A). A caveat to our experiments is that quantitatively measuring active PARs is technically difficult due to the limited range of experimental tools that are available for studying these receptors. However, fluorescence imaging of FLAG-tagged PAR1 and PAR2 by confocal microscopy (Supplemental Fig. 1C) shows that a substantial portion of total expressed receptors localize at the plasma membrane, and other studies (Figs. 1-5) confirm that some fraction of these receptors is functional. PAR1 and PAR2 are recovered by anti-FLAG antibodies covalently coupled to agarose beads, and can be detected by immunoblot analysis (Supplemental Fig. 1B). Both receptors are readily recovered and migrate upon being subjected to SDS-PAGE and appear as a prominent smear on western blots. The reason for this smearing is unknown, but may be due to receptor glycosylation and/or aggregation (as is the case with ectopic expression of many recombinant GPCRs). However, quantification of active receptors remains challenging, and we can only make qualitative statements about PAR amounts and

Molecular Pharmacology Fast Forward. Published on March 9, 2010 as DOI: 10.1124/mol.109.062018
This article has not been copyedited and formatted. The final version may differ from this version.

recovery. With these limitations in mind, we initiated experiments using expressed PAR1 and PAR2 with specific Gα proteins in COS-7 cells to compare PAR1 and PAR2 signaling.

Depending on the cell type being studied, both PAR1 and PAR2 are reported to activate one or more isoforms of phospholipase C (PLC) to initiate phosphatidylinositol (4,5)-bisphosphate hydrolysis and InsP signaling (Hung et al., 1992;Dery et al., 1998;Hains et al., 2006). To determine whether PAR1 and PAR2 stimulated PLC activity in COS-7 cells, we measured accumulation of radiolabeled InsPs in cells transfected with either PAR1 or PAR2 in response to each PAR-AP--TFLLR or LIGRLO (Fig. 1A). Consistent with previous reports, both receptors stimulated measurable InsP production whereas control cells transfected with the empty pcDNA3.1 vector did not (Fig. 1A).

We also examined whether PAR1 and PAR2 stimulate calcium mobilization. The amphibian *X. laevis* oocytes express calcium-activated chloride currents that provide a simple and sensitive readout of $G_{q/11}$-simulated mobilization of intracellular calcium (Dascal and Cohen, 1987;Mannaioni et al., 2008;Oron et al., 1985;Nystedt et al., 1994). We found that oocytes injected with PAR1 or PAR2 cRNA and stimulated with the appropriate PAR-AP increase the activity of calcium-activated chloride channels. At a holding potential of -40 mV, separate activation of PAR1 and PAR2 evokes an inward current characteristic of the calcium-activated chloride channel, indicating that both PAR1 and PAR2 mobilize intracellular calcium in response to InsP production. Using mock-injected oocytes as controls, we found that these cells did not evoke an inward current in response to stimulation with PAR-APs, as expected (Fig. 1B).

PARs also have been reported to activate MAPK pathways and stimulate ERK1/2 phosphorylation (Kramer et al., 1995;DeFea et al., 2000). Various G proteins (G_s, $G_{q/11}$, $G_{i/o}$) initiate signaling pathways that converge on ERK1/2 (DeFea et al., 2000;Ramachandran et al., 2009), and it is well established that $G_{i/o}$-linked pathways activate ERK1/2 phosphorylation by release of Gβγ, in a PTX-sensitive manner (Gerhardt et al., 1999). Our lab and others have

Molecular Pharmacology Fast Forward. Published on March 9, 2010 as DOI: 10.1124/mol.109.062018
This article has not been copyedited and formatted. The final version may differ from this version.

shown that MAPK signaling stimulated by PARs contributes to the proliferation of a number of different cell types including astrocytes (Sorensen et al., 2003;Wang et al., 2002). Here we confirm that in COS-7 cells expressing recombinant PARs, ERK1/2 phosphorylation is elicited by each of their receptor-specific PAR-APs. No response to agonist stimulation occurs with either of the PAR-APs when cells are transfected with vector alone (Fig. 1C).

A third G protein-linked pathway that is reported to be activated by PARs is Rho signaling, which is known to be mediated primarily through the $G_{12/13}$ family (Offermanns et al., 1994;Post et al., 1996;Aragay et al., 1995) but also can be activated through $G_{q/11}$ stimulation of p63RhoGEF (Lutz et al., 2005). Previous studies have shown that PAR1 and PAR2 activation of Rho triggers cellular responses including cellular proliferation, migration, and morphological changes, including platelet shape change, neurite retraction, and growth cone collapse (Klages et al., 1999;Citro et al., 2007;Nurnberg et al., 2008). To determine whether PAR1 and PAR2 also activate this pathway in COS-7 cells, we employed a chemiluminescence-based ELISA Rho assay system that relies on the Rho-binding domain of Rho effector proteins to detect formation of Rho-GTP from cell lysates. We found that the levels of activated RhoA-GTP is increased approximately 3- and 2.5-fold over basal, respectively, following stimulation of PAR1 or PAR2 with the appropriate PAR-AP (Fig. 1D). Taken together, these findings indicate that both PAR1 and PAR2 functionally couple to multiple G protein regulated pathways in COS-7 cells.

PAR1 and PAR2 form stable complexes with both overlapping and distinct sets of G proteins—Although functional PAR coupling to $G_{q/11}$-, $G_{i/o}$-, and $G_{12/13}$-linked signaling pathways has been reported previously (and confirmed here), only very limited information is available regarding direct PAR complex formation with individual G protein family members. Therefore, we screened members of each of these candidate G protein subfamilies ($G_{q/11}$, $G_{i/o}$ and $G_{12/13}$) for their capacities to form a stable complex (i.e., recovered by co-IP) with PAR1 or with PAR2

Molecular Pharmacology Fast Forward. Published on March 9, 2010 as DOI: 10.1124/mol.109.062018
This article has not been copyedited and formatted. The final version may differ from this version.

(Fig. 2). Carboxy-terminally FLAG-tagged PAR1 or PAR2 and individual Gα protein subunits were each independently co-expressed as PAR/G protein pairs in COS-7 cells. The FLAG-tagged α_{1A}-adrenergic receptor (α_{1A}-AR), which is known to be $G_{q/11}$-linked, was compared in parallel with the PARs as a control. In addition, β_2-AR, a G_s linked receptor, was also evaluated for its capacity to bind to $G\alpha_s$, $G\alpha_{11}$, $G\alpha_o$ and $G\alpha_{12}$ (Supplemental Fig. 2). Anti-FLAG agarose beads were used to recover the receptor/G protein complexes (as in Supplemental Fig. 1B), and samples were analyzed for the presence of the G protein in the recovered material (IP, Fig. 2 top) and in the lysate (input, Fig. 2 bottom). We found that PAR1 and PAR2 couple to overlapping and distinct sets of G proteins. Little or no detectable G proteins are recovered when only the individual G proteins and control vector are transfected into cells in the absence of receptor expression (Fig. 2, bottom row, top panel). All of the tested $G\alpha_{q/11}$ family members ($G\alpha_q$, $G\alpha_{11}$, $G\alpha_{14}$) and the $G\alpha_{12}$ family members ($G\alpha_{12}$, $G\alpha_{13}$) formed a stable complex with PAR1 and PAR2, as well as with α_{1A}-AR; each of these G protein subunits bound to similar extents to both PAR1 and PAR2, which were recovered at comparable levels (Supplemental Fig. 1B). In stark contrast, all of the $G\alpha_{i/o}$ subunits (except $G\alpha_{i3}$) bound to PAR1, but only weakly or not at all to PAR2 or to α_{1A}-AR. Of note, much more of the $G\alpha_o$ subunit appears to have bound to PAR1 than any other Gα subunits tested (Fig. 2). Whether this binding reflects a more robust coupling is uncertain since the Gα-specific antibodies differ in their relative staining intensities. Therefore, we can only make qualitative statements about PAR/G protein coupling from these data.

To further test the specificity of these apparent interactions, we compared PAR1/G protein coupling with the G_s-coupled β_2-AR (Supplemental Fig. 2). As expected, β_2-AR bound to $G\alpha_s$ but *not* to $G\alpha_o$ or $G\alpha_{12}$, whereas PAR1 bound to $G\alpha_o$, $G\alpha_{11}$ and $G\alpha_{12}$ (as before) but *not* to $G\alpha_s$. We also observe a small amount of $G\alpha_{11}$ that co-eluted with β_2-AR. Since β_2-AR is not reported to activate $G_{q/11}$-linked pathways, we believe this interaction (possibly non-specific)

Molecular Pharmacology Fast Forward. Published on March 9, 2010 as DOI: 10.1124/mol.109.062018
This article has not been copyedited and formatted. The final version may differ from this version.

does not reflect functional coupling. Apart from this observation, all of the PAR/G protein complexes we identified seem real and reflect previous reports of functional coupling. To our knowledge, these data are the first to demonstrate stable interactions between PARs and a wide variety of Gα proteins and identifies clear differences between PAR1 and PAR2 G protein coupling. Of particular note, PAR1, but not PAR2 couples to specific $G_{i/o}$ family members.

PAR1 and PAR2 form stable complexes with G protein heterotrimers— In our screens for receptor/G protein pairs, no agonist was added to the cells to either promote or disrupt the complexes. Therefore, we examined the effects of PAR-APs and activating guanine nucleotide on the formation and stability of PAR/Gα complexes. Furthermore, we tested whether PARs interacted with G protein heterotrimers (Gαβγ) as determined by the presence of Gβ in the recovered complex. Protein complexes were recovered from COS-7 cell lysates expressing PAR/G proteins as described above (Fig. 2). Specifically, we examined the effects of agonist and activating nucleotide (GTPγS) on PAR1 and PAR2 interactions with either G_{11} or G_o in cell lysates. COS-7 cell lysates containing both membranes and cytosol were incubated either alone or in the presence of agonist and 10 μM GTPγS for 30 min. Following co-IP, we found that PAR1 was recovered in complex with both G_{11} and G_o, and PAR2 with only G_{11} (Fig. 3), as before. Of note, endogenous Gβ (and likely Gγ, though not tested) subunits also were present in the recovered complexes, presumably in a heterotrimeric complex with recombinant Gα. Somewhat surprisingly, no differences in PAR/G_o or PAR/G_{11} complexes were elicited by addition of PAR-APs and GTPγS (Fig. 3).

PAR1 selectively couples to $G_{i/o}$ *signaling pathways*—Thus far, our findings have identified a difference between PAR1 and PAR2 interactions with $G_{i/o}$ family members. Because we showed that PAR1 but not PAR2 physically couples with $G\alpha_{i/o}$ subunits, we investigated whether there were functional differences in PAR activation of $G_{i/o}$-mediated

Molecular Pharmacology Fast Forward. Published on March 9, 2010 as DOI: 10.1124/mol.109.062018
This article has not been copyedited and formatted. The final version may differ from this version.

intracellular signaling pathways in COS-7 cells. To do so, we tested the role of PARs in the $G_{i/o}$-mediated inhibition of β_2-AR-induced cAMP accumulation and in the $G_{i/o}$-mediated stimulation of ERK1/2 phosphorylation (Fig. 4). Measurements of cellular cAMP were performed in COS-7 cells transiently expressing either PAR1 or PAR2 following stimulation with isoproterenol alone or in combination with either PAR-AP. PTX-sensitivity also was determined as a measure of $G_{i/o}$ involvement. In cells expressing either PAR1 or PAR2, isoproterenol elicited high levels of cAMP production, which indicates that the β-AR is also present in these cells. When cells were stimulated in parallel with TFLLR, cellular cAMP levels were significantly reduced by 20-25% (p = 0.012; Fig. 4A), and this inhibition is reversed by pretreatment of cells with PTX. By contrast, LIGRLO does not reduce isoproterenol-stimulated cAMP production in PAR2-expressing COS-7 cells, nor is this response affected by PTX (Fig. 4B).

Activation of $G_{i/o}$-linked pathways also stimulates MAPK signaling. Therefore, we also measured ERK1/2 phosphorylation experiments in COS-7 cells expressing either PAR1 or PAR2, in the presence or absence of PTX treatment. Preliminary studies indicated that both PAR1 and PAR2 maximally stimulated ERK1/2 phosphorylation following a 2 min activation with the appropriate PAR-AP (data not shown). Cells expressing either PAR1 or PAR2 were pretreated with increasing concentrations of PTX overnight, and then stimulated with PAR-APs. Of note, the PAR1-induced ERK1/2 phosphorylation response was reduced to control levels (cells transfected with vector but stimulated with PAR-AP) by PTX pretreatment whereas the ERK1/2 phosphorylation elicited by PAR2 remained unchanged (Fig. 4C-D). For both PAR1 and PAR2, total ERK1/2 levels remained the same for all conditions. Taken together, our data showing PTX-sensitivity of TFLLR effects on cAMP accumulation and ERK1/2 phosphorylation indicate that PAR1 signaling responses in COS-7 cells rely, in part, on $G_{i/o}$ activation, whereas the parallel PAR2-mediated signaling responses do not. Our findings here with functional assays are consistent with our biochemical data above (Fig. 2), and together these findings

Molecular Pharmacology Fast Forward. Published on March 9, 2010 as DOI: 10.1124/mol.109.062018
This article has not been copyedited and formatted. The final version may differ from this version.

show that PAR1, but not PAR2, forms a stable functional complex with $G_{i/o}$ proteins to selectively activate linked pathways in COS-7 cells.

PAR1 and PAR2 both utilize $G_{q/11}$ and $G_{12/13}$ to activate PLC and Rho, respectively— Besides PAR1-$G_{i/o}$ interactions, our findings (Fig. 2) also show that both PAR1 and PAR2 complex with $G_{q/11}$ and $G_{12/13}$ family members and activate pathways linked to these G proteins (Fig. 1). Therefore, we investigated whether PAR1 and PAR2 activated inositol lipid and RhoA signaling by employing inhibitors of select G proteins in COS-7 cells. For these studies, we utilized GRK2-RGS and p115-RGS, which bind directly to and specifically inhibit signaling by $G_{q/11}$ and $G_{12/13}$, respectively (Hains et al., 2006). COS-7 cells were separately transfected with either PAR1 or PAR2 alone or together with either GRK2-RGS or p115-RGS. Cells then were challenged with the appropriate PAR-AP and either InsP accumulation or active RhoA-GTP was measured as before (Fig. 1). RhoA activation was measured in cells expressing PAR1 or PAR2 alone or in combination with p115-RGS. Whereas the PAR1-AP and PAR2-AP both stimulated RhoA activation two-fold over basal, this response was reduced to basal levels in the presence of p115-RGS (Fig. 5A), indicating that RhoA activation by PARs relies on $G_{12/13}$ activation (in these cells using these methods). By contrast, activation of InsPs by PAR1 and by PAR2 in COS-7 cells appears to be mediated by $G_{q/11}$ (Fig. 5B). We found that both of the PAR-APs stimulated maximal InsPs in the presence or absence of p115-RGS (Fig. 5B). Since both $G_{q/11}$ and $G_{12/13}$ stimulate inositol lipid signaling by distinct PLC iosforms (PLC-β and PLC-ε, respectively), we tested inhibitors of both G proteins. The PAR-activated responses were reduced by approximately 85% and 65% of maximal InsP production, respectively, in cells that expressed GRK2-RGS (Fig. 5B) suggesting that both PAR1- and PAR2-directed InsP production in COS-7 cells is mediated predominantly by $G_{q/11}$ (and likely PLC-β) and not by $G_{12/13}$ (and PLC-ε) under these experimental conditions.

Molecular Pharmacology Fast Forward. Published on March 9, 2010 as DOI: 10.1124/mol.109.062018
This article has not been copyedited and formatted. The final version may differ from this version.

PAR-stimulated cAMP, PLC and RhoA signaling in Neu7 cells

Up to this point, we have compared PAR1 and PAR2 coupling to G proteins by examining recombinant proteins exogenously expressed in cells that express undetectable levels of functional PARs (COS-7 cells). These studies (Figs. 1-5) have been valuable in identifying both similarities and differences between these two closely related receptors. However, in order to confirm the physiological relevance of these observations, we deemed it necessary to determine whether these differences in PAR/G protein coupling and signaling are maintained in cells that endogenously express these proteins. For this purpose, we obtained Neu7 astrocytes, a cell line reported to express both native PAR1 and PAR2 (Vandell et al., 2008).

We first tested whether endogenous PAR1 and PAR2 both activate the same G protein signaling pathways in Neu7 cells as we observed with recombinant proteins in COS-7 cells (Fig. 6). Since these cells do not transfect well, we employed PTX and selective pharmacological inhibitors of PLCβ (U73122) and RhoA (C3 toxin) to dissect the involved downstream signaling pathways. Cellular cAMP levels were measured in Neu7 cells following stimulation of an endogenous β-AR with isoproterenol alone or in combination with either TFLLR or LIGRLO. As shown in Figure 6A, isoproterenol stimulated cAMP production. Upon simultaneous activation with isoproterenol and TFLLR, cellular cAMP levels were reduced by nearly 40% (p =0.035), and this inhibition is reversed in the presence of PTX. Conversely, LIGRLO in the presence or absence of PTX had no effect on cAMP production in Neu7 cells (Fig. 6A). TFLLR- or LIGRLO-stimulated InsP accumulation or RhoA-GTP formation also was measured as before (Fig. 1 and Fig. 5). We found that both of the PAR-APs stimulated InsPs in the presence or absence of C3 toxin (Fig. 6B), suggesting no role for $G_{12/13}$-linked Rho pathways. However, this PAR-activated response was reduced to approximately basal levels of InsP production in cells treated with

Molecular Pharmacology Fast Forward. Published on March 9, 2010 as DOI: 10.1124/mol.109.062018
This article has not been copyedited and formatted. The final version may differ from this version.

U73122 (Fig. 6B), indicating that both PAR1- and PAR2-mediated InsP production in Neu7 cells is activated by a $G_{q/11}$-PLC pathway under these conditions. Conversely, PAR1 and PAR2 activation of RhoA in Neu7 cells (Fig. 6C) is likely mediated by $G_{12/13}$-RhoA pathways since both PAR-APs activated RhoA. This activation was reversed to near basal levels in the presence of C3 toxin (Fig. 6C).

PAR1 and PAR2 utilize overlapping and distinct G protein pathways to stimulate ERK1/2 phosphorylation in Neu7--Because our studies in COS-7 cells indicate that PAR1 selectively couples to $G_{i/o}$ to activate ERK1/2 signaling (Figs. 2-4), and PAR1 inhibition of cAMP production in Neu7 cells is PTX-sensitive, we sought to determine whether PAR1 activation of ERK1/2 in Neu7 cells relied on $G_{i/o}$ signaling as well (Fig. 7). Neu7 cells were treated with varying concentrations of PTX (0-300 ng/mL) overnight and then separately stimulated with the PAR-APs. Cells were harvested and levels of ERK1/2 phosphorylation, normalized to total ERK levels, were measured by immunoblot analysis (Fig. 7A) and quantified by densitometry (Fig. 7B). PTX treatment inhibited TFLLR-stimulated ERK1/2 phosphorylation in Neu7 cells (greater than 50%) when compared to the effects of LIGRLO. This inhibition was statistically significant (Fig. 7B; p <0.001) across all PTX concentrations tested, independent of the concentration of toxin used. By contrast, PTX had no effect on LIGRLO-directed ERK signaling. These findings with endogenous proteins in native cells are consistent with our studies in COS-7 cells (Figs. 2-4), which show that PAR1, but not PAR2, forms a functional complex with $G_{i/o}$ family members, and that PAR1, but not PAR2 relies on $G_{i/o}$ to stimulate ERK1/2 phosphorylation.

To determine the mechanism whereby PAR2 elicits ERK1/2 phosphorylation, we employed inhibitors of various other signaling pathways known to be involved in ERK1/2 signaling. Neu7 cells were treated with PAR-APs together with either no inhibitor, the selective PKC inhibitor BIS, the selective PLCβ inhibitor U73122, or the Rho inhibitor C3 toxin. Cells were harvested and ERK1/2 phosphorylation levels were assessed through immunoblot analyses

Molecular Pharmacology Fast Forward. Published on March 9, 2010 as DOI: 10.1124/mol.109.062018
This article has not been copyedited and formatted. The final version may differ from this version.

followed by densitometry (Fig. 7C-D). Pretreatment of cells with the PLC inhibitor, U73122, but not inhibitors of PKC or Rho signaling, reduced TFLLR- and LIGRLO-stimulated ERK1/2 phosphorylation levels nearly half (p <0.05 and p <0.01, respectively; Fig. 7C), suggesting that PAR1 and PAR2 both (partially) stimulate ERK1/2 signaling through PLC-mediated pathways (Fig. 7C-D). However, as shown above, $G_{i/o}$-mediated pathways also contribute to ERK1/2 phosphorylation mediated by PAR1 but not by PAR2 (Fig. 7A-B).

PAR1, but not PAR2, influences Neu7 cell migration via a PTX-sensitive $G_{i/o}$ pathway— ERK1/2 pathways regulate cell growth, proliferation, and migration among other cellular processes. To provide a physiological readout of the activation of $G_{i/o}$-linked pathways by PARs, we tested whether PAR-APs modulated cellular migration of Neu7 cells as measured by a wound-scratch assay (Fig. 8). For these experiments, cells were plated and grown to 100% confluence, after which a scratch across the monolayer was introduced resulting in a space devoid of cells. In this assay, migration of cells into the empty space after 24 h in response to agonist is a measure of cell migration. Cells were placed in serum-free media containing either vehicle, TFLLR, or LIGRLO in the presence or absence of PTX or the ERK (MEK1/2) inhibitor U0126. In the absence of serum or PAR-APs (control), Neu7 astrocytes exhibited some migration into the empty space after 24 h, consistent with basal movement of these cells. TFLLR and LIGRLO both stimulated clearly evident migration compared to control cells, nearly filling the space (Fig. 8A-B). However, following PTX treatment, only TFLLR-directed Neu7 cell migration is significantly blocked (p =0.03) whereas cell migration associated with LIGRLO or vehicle treatment was unaffected (Fig. 8A-B). We believe that the presence of PAR-AP-stimulated cells in the wounded area is indicative of migration and not cellular proliferation because Neu7 cells grown and treated identically failed to incorporate [^{3}H]thymidine into new DNA synthesis, a measure of cellular proliferation (Fig 8C).

Interestingly, the MEK inhibitor U0126 significantly blocks cell migration by PAR1 (p =0.003) and PAR2 (p =0.04), respectively, indicating that both receptors rely on ERK1/2

Molecular Pharmacology Fast Forward. Published on March 9, 2010 as DOI: 10.1124/mol.109.062018
This article has not been copyedited and formatted. The final version may differ from this version.

signaling pathways to promote cell migration. To further characterize the mechanism by which PAR2 induces cell migration, we attempted to perform the same wound-scratch experiments in the presence of the PLC inhibitor (U73122) that blocks PAR2-mediated ERK1/2 phosphorylation (Fig. 7C-D). However, after 24 h, very few cells treated with U73122 remained adhered to the plate, indicating that long-term treatment with this inhibitor is toxic to Neu7 cells, thereby limiting our capacity to measure PLC-effects on PAR-mediated cell migration in Neu7 cells.

Molecular Pharmacology Fast Forward. Published on March 9, 2010 as DOI: 10.1124/mol.109.062018
This article has not been copyedited and formatted. The final version may differ from this version.

Discussion

Although much has been learned about PAR1 signaling in recent years, substantially less is known about PAR2 signaling. Furthermore, only one study has compared PAR1- and PAR2-directed G protein signaling in the same cells (olfactory sensory neurons of the olfactory bulb) (Olianas et al., 2007). Here we compared PAR1 and PAR2 signaling in COS-7 cells that express undetectable levels of these PAR receptors, and also in Neu7 astrocytes that natively express both receptors. Our key findings indicate the following: 1) PAR1 and PAR2 couple to both overlapping and distinct sets of G proteins; 2) PAR1 but not PAR2 links to G_o and G_i family members; 3) Receptor/G protein complex formation is stable even in the presence of activating ligand and nucleotide; 4) $G_{i/o}$ contributes to PAR1- but not PAR2-directed effects on cellular ERK1/2 and cAMP signaling in both COS-7 cells and Neu7 cells; 5) PAR1, but not PAR2 relies partly on a PTX-sensitive $G_{i/o}$ signaling pathway to stimulate ERK1/2 signaling and cell migration in Neu7 cells; and 6) both PAR1 and PAR2 rely partly on $G_{q/11}$-PLC signaling pathways to stimulate ERK1/2 signaling and cell migration in Neu7 cells. We will discuss each of these findings.

PAR1 and PAR2 both couple to multiple overlapping sets of G proteins

Our findings indicate that PAR1 and PAR2 both couple, to similar extents, to $G_{q/11}$ family members (G_q, G_{11} and G_{14}), $G_{12/13}$ family members (G_{12} and G_{13}) and to the downstream signaling pathways activated by these G proteins. These signaling pathways include InsP production, calcium signaling, and RhoA activation. In COS-7 cells, the former signaling response likely is due to activation of PLC-β, but not PLC-ε, since a direct and selective inhibitor of $G_{12/13}$ did not affect InsP accumulation. Our findings also suggest that in COS-7 cells, PAR1 and PAR2 activation of RhoA is mediated by $G_{12/13}$ since a direct and selective inhibitor of $G_{12/13}$ reduced RhoA activation to near basal levels in response to activation of either receptor. Which G protein signaling pathway PARs choose to utilize in order to activate either InsP/calcium

Molecular Pharmacology Fast Forward. Published on March 9, 2010 as DOI: 10.1124/mol.109.062018
This article has not been copyedited and formatted. The final version may differ from this version.

and/or RhoA likely is cell-specific since cross-talk between these G protein-linked pathways is known to occur (Hains et al., 2006;Citro et al., 2007;Kelley et al., 2004).

PAR1, but not PAR2, couples to G_o and also to G_i family members

Our results indicate that PAR1, but not PAR2, is coupled to G_o and to G_i family members (G_{i1} and G_{i2}). In our studies, we assessed receptor/G protein complex formation, inhibition of adenylyl cyclase-directed cAMP production, and PTX-sensitive ERK1/2 activation. These findings are consistent with previous reports indicating that PAR1-directed PI3K signaling and platelet activation is mediated by PTX-sensitive $G_{i/o}$ signaling (Voss et al., 2007), that PAR1 pre-assembles with G_{i1} in bioluminescence resonance energy transfer studies (Ayoub et al., 2007), and that G_o mediates PAR1-directed intracellular calcium signaling and cytoskeletal rearrangements in endothelial cells (Vanhauwe et al., 2002). Significantly, our findings suggest that, at least in the cells examined in these studies, PAR2 does not couple to G_o or to G_i family members. This difference in G protein coupling could have profound consequences for the physiological responses of cells that express both PAR1 and PAR2.

Our findings raise the important mechanistic question of how PAR's couple to multiple distinct G proteins. The intracellular loops 2, 3 and 4 of PAR1 have been implicated in receptor-G protein coupling (Verrall et al., 1997;Swift et al., 2006). These loops are relatively small and are not likely to couple to three or more G proteins simultaneously due to steric hindrance alone. One possibility is that different populations of PARs may link to distinct G proteins depending on receptor location within the plasma membrane, as is the case with the $S1P_1$ receptor. Like PARs, the $S1P_1$ receptor is a GPCR that links to multiple G protein signaling pathways (Means et al., 2008;Sorensen et al., 2003). Recent studies show that $S1P_1$ receptor coupling to specific G proteins depends on whether or not the receptor is localized to lipid rafts (caveolae) (Means et al., 2008). Perhaps PAR-G protein coupling also depends on receptor localization within specialized microdomains of the plasma membrane. A separate question centers on whether

Molecular Pharmacology Fast Forward. Published on March 9, 2010 as DOI: 10.1124/mol.109.062018
This article has not been copyedited and formatted. The final version may differ from this version.

PARs contain specific recognition sites for each G protein or, alternatively, whether multiple G proteins dock at overlapping recognition sites. Ongoing studies in our laboratory are investigating these two possibilities. We also should note that the agonists we used in our experiments could influence the G protein coupling of the PARs. McLaughlin and colleagues (McLaughlin et al., 2005) have shown that different agonists for the same receptor (PAR1) exhibit a functional selectivity for particular G protein pathways. That is, PAR-APs, rather than endogenous agonists (e.g., thrombin), cause PAR1 to couple much more strongly to $G_{q/11}$ signaling pathways relative to $G_{12/13}$ signaling pathways (McLaughlin et al., 2005). However, this finding does not explain the PAR/G protein complexes we observed that formed *independent* of receptor agonist, and our biochemical data are consistent with PAR/G signaling events we observed in both cells types using the PAR-APs.

PAR1 and PAR2 form complexes with G proteins that are stable in the presence of agonist and nucleotide

We found that PAR1 and PAR2 both form stable complexes with G protein heterotrimers (i.e., $G\alpha_{11}$ plus $G\beta\gamma$, as well as $G\alpha_o$ plus $G\beta\gamma$) that remain intact in cell lysates following addition of agonist and activating nucleotide (e.g., GTPγS). These findings were unexpected since most established models of GPCR/G protein signaling and many previous reports suggest that agonist and nucleotide activation of GPCRs results in dissociation of the receptor/G protein complex. One possibility is that PAR/G complexes behave differently in broken cell lysates versus whole cells (i.e., missing intact cellular elements that are necessary for uncoupling). Alternatively, these findings also are consistent with more recent reports and proposed models, which suggest that the receptor/G protein complex remains intact following agonist activation. In this new model, receptors serve as signaling platforms that assemble multiple signaling components (e.g., heterotrimeric G proteins, RGS proteins, arrestins, GRKs, effectors) and,

Molecular Pharmacology Fast Forward. Published on March 9, 2010 as DOI: 10.1124/mol.109.062018
This article has not been copyedited and formatted. The final version may differ from this version.

following receptor activation, G proteins do not dissociate but instead rearrange *in situ* to initiate signaling (Bunemann et al., 2003;Hein and Bunemann, 2008). Whether these receptor/G protein complexes internalize as a complex is unknown, though sustained coupling following internalization could result in sustained G protein signaling since PARs are constitutively activated following protease cleavage. Sustained PAR/G protein complex formation also is consistent with evidence showing that PAR-mediated ERK1/2 activation differs from some other GPCRs (DeFea et al., 2000). In the case of PAR2, ERK1/2 phosphorylation is partially dependent on formation of a stable PAR2/Arrestin2 (Arr2) complex that directs ERK signals away from the nucleus and cellular proliferation. However, uncoupling PAR2 from Arr2 binding results in ERK1/2 signaling that is directed to the nucleus to promote cell proliferation (DeFea et al., 2000). Of note, our findings with ERK activation (Figs. 4 and 7) likely reflect initial PAR2/G protein activation (i.e., 2 min of stimulation) of $G_{q/11}$-PLC-mediated pathways rather than PAR2/Arrestin signaling (under these experimental conditions in Neu7 cells).

$G_{i/o}$ signaling mediates PAR1 but not PAR2 contributions to ERK1/2 signaling and migration in Neu7 astrocytes

We observed that PTX treatment had differential effects on PAR1 and PAR2 signaling and cellular responses in Neu7 cells. Both PAR1 and PAR2 stimulated ERK1/2 phosphorylation and cell migration but only PAR1 effects on MAPK signaling and migration were PTX-sensitive. By contrast, PLC signaling pathways contribute to both PAR1- and PAR2-directed ERK1/2 phosphorylation and Neu7 cell migration. Importantly, cell migration induced by both PARs appears to rely on ERK signaling. The MEK1/2 inhibitor U0126 significantly reduced migration observed when either PAR-AP was used to stimulate migration into the open area of the cell monolayer. Whether this finding is consistent with the mechanism by which PAR2 activates ERK1/2 signaling (i.e., through PLC-mediated pathways) remains unknown. Our attempts to fully characterize the mechanism responsible for PAR2-directed cell migration were

Molecular Pharmacology Fast Forward. Published on March 9, 2010 as DOI: 10.1124/mol.109.062018
This article has not been copyedited and formatted. The final version may differ from this version.

unsuccessful since we found that the PLC inhibitor U73122 is extremely toxic to Neu7 cells after 24 h time period required for the studies. Nevertheless, our cell migration data in cells expressing native PARs and G proteins corroborate our observations with recombinant proteins in COS-7 cells–that PAR1 selectively couples to $G_{i/o}$ whereas PAR2 does not. Neu7 cells have been used as a cell culture-based model system to study mechanisms of glial scarring (Fok-Seang et al., 1995). As such, PAR1- and PAR2-directed signaling pathways may interact differentially with those of other CNS-derived factors to modulate cell growth and proliferation involved with glial scarring following head injury, stroke or other insults that compromise the blood-brain barrier.

In summary, we report here that PAR1 and PAR2 activate multiple shared and distinct G protein signaling pathways, and that PAR1, but not PAR2, relies upon G_o and G_i family members to mediate its receptor-specific effects on MAPK signaling and cell migration. These studies highlight previously unknown G protein signaling mechanisms used by these two closely related receptors, and physiologically relevant differences between them.

Acknowledgements

The authors would like to Christopher Vellano for his technical assistance with confocal imaging studies and for thoughtful discussions regarding this manuscript. We also thank Dr. Joann Trejo (University of California, San Diego) for kind input and advice and all members of the Traynelis laboratory for helpful assistance and guidance.

Molecular Pharmacology Fast Forward. Published on March 9, 2010 as DOI: 10.1124/mol.109.062018
This article has not been copyedited and formatted. The final version may differ from this version.

References

Aragay AM, Collins L R, Post G R, Watson A J, Feramisco J R, Brown J H and Simon M I (1995) G12 Requirement for Thrombin-Stimulated Gene Expression and DNA Synthesis in 1321N1 Astrocytoma Cells. *J Biol Chem* **270**:20073-20077.

Ayoub MA, Maurel D, Binet V, Fink M, Prezeau L, Ansanay H and Pin J P (2007) Real-Time Analysis of Agonist-Induced Activation of Protease-Activated Receptor 1/Galphai1 Protein Complex Measured by Bioluminescence Resonance Energy Transfer in Living Cells. *Mol Pharmacol* **71**:1329-1340.

Blackhart BD, Ruslim-Litrus L, Lu C C, Alves V L, Teng W, Scarborough R M, Reynolds E E and Oksenberg D (2000) Extracellular Mutations of Protease-Activated Receptor-1 Result in Differential Activation by Thrombin and Thrombin Receptor Agonist Peptide. *Mol Pharmacol* **58**:1178-1187.

Bunemann M, Frank M and Lohse M J (2003) Gi Protein Activation in Intact Cells Involves Subunit Rearrangement Rather Than Dissociation. *Proc Natl Acad Sci U S A* **100**:16077-16082.

Citro S, Malik S, Oestreich E A, Radeff-Huang J, Kelley G G, Smrcka A V and Brown J H (2007) Phospholipase Cepsilon Is a Nexus for Rho and Rap-Mediated G Protein-Coupled Receptor-Induced Astrocyte Proliferation. *Proc Natl Acad Sci U S A* **104**:15543-15548.

Coughlin SR (2005) Protease-Activated Receptors in Hemostasis, Thrombosis and Vascular Biology. *J Thromb Haemost* **3**:1800-1814.

Dascal N and Cohen S (1987) Further Characterization of the Slow Muscarinic Responses in Xenopus Oocytes. *Pflugers Arch* **409**:512-520.

DeFea KA, Zalevsky J, Thoma M S, Dery O, Mullins R D and Bunnett N W (2000) Beta-Arrestin-Dependent Endocytosis of Proteinase-Activated Receptor 2 Is Required for Intracellular Targeting of Activated ERK1/2. *J Cell Biol* **20;148**:1267-1281.

Dery O, Corvera C U, Steinhoff M and Bunnett N W (1998) Proteinase-Activated Receptors: Novel Mechanisms of Signaling by Serine Proteases. *Am J Physiol* **274**:C1429-C1452.

Fok-Seang J, Smith-Thomas L C, Meiners S, Muir E, Du J S, Housden E, Johnson A R, Faissner A, Geller H M, Keynes R J and . (1995) An Analysis of Astrocytic Cell Lines With Different Abilities to Promote Axon Growth. *Brain Res* **689**:207-223.

Gerhardt CC, Gros J, Strosberg A D and Issad T (1999) Stimulation of the Extracellular Signal-Regulated Kinase 1/2 Pathway by Human Beta-3 Adrenergic Receptor: New Pharmacological Profile and Mechanism of Activation. *Mol Pharmacol* **55**:255-262.

Hains MD, Siderovski D P and Harden T K (2004) Application of RGS Box Proteins to Evaluate G-Protein Selectivity in Receptor-Promoted Signaling. *Methods Enzymol* **389:71-88.**:71-88.

Hains MD, Wing M R, Maddileti S, Siderovski D P and Harden T K (2006) Galpha12/13- and Rho-Dependent Activation of Phospholipase C-Epsilon by Lysophosphatidic Acid and Thrombin Receptors. *Mol Pharmacol* **69**:2068-2075.

Hamill CE, Mannaioni G, Lyuboslavsky P, Sastre A A and Traynelis S F (2009) Protease-Activated Receptor 1-Dependent Neuronal Damage Involves NMDA Receptor Function. *Exp Neurol* **217**:136-146.

Hein P and Bunemann M (2008) Coupling Mode of Receptors and G Proteins. *Naunyn Schmiedebergs Arch Pharmacol*.

Hung DT, Wong Y H, Vu T K and Coughlin S R (1992) The Cloned Platelet Thrombin Receptor Couples to at Least Two Distinct Effectors to Stimulate Phosphoinositide Hydrolysis and Inhibit Adenylyl Cyclase. *J Biol Chem* **267**:20831-20834.

Ishihara H, Connolly A J, Zeng D, Kahn M L, Zheng Y W, Timmons C, Tram T and Coughlin S R (1997) Protease-Activated Receptor 3 Is a Second Thrombin Receptor in Humans. *Nature* **386**:502-506.

Kelley GG, Reks S E and Smrcka A V (2004) Hormonal Regulation of Phospholipase Cepsilon Through Distinct and Overlapping Pathways Involving G12 and Ras Family G-Proteins. *Biochem J* **378**:129-139.

Klages B, Brandt U, Simon M I, Schultz G and Offermanns S (1999) Activation of G12/G13 Results in Shape Change and Rho/Rho-Kinase-Mediated Myosin Light Chain Phosphorylation in Mouse Platelets. *J Cell Biol* **144**:745-754.

Kramer RM, Roberts E F, Hyslop P A, Utterback B G, Hui K Y and Jakubowski J A (1995) Differential Activation of Cytosolic Phospholipase A2 (CPLA2) by Thrombin and Thrombin Receptor Agonist Peptide in Human Platelets. Evidence for Activation of CPLA2 Independent of the Mitogen-Activated Protein Kinases ERK1/2. *J Biol Chem* **270**:14816-14823.

Lutz S, Freichel-Blomquist A, Yang Y, Rumenapp U, Jakobs KH, Schmidt M and Wieland T (2005) The Guanine Nucleotide Exchange Factor P63RhoGEF, a Specific Link Between Gq/11-Coupled Receptor Signaling and RhoA. *J Biol Chem* **280**.

Macfarlane SR, Seatter M J, Kanke T, Hunter G D and Plevin R (2001) Proteinase-Activated Receptors. *Pharmacol Rev* **53**:245-282.

Mannaioni G, Orr A G, Hamill C E, Yuan H, Pedone K H, McCoy K L, Berlinguer P R, Junge C E, Lee C J, Yepes M, Hepler J R and Traynelis S F (2008) Plasmin Potentiates Synaptic N-Methyl-D-Aspartate Receptor Function in Hippocampal Neurons Through Activation of Protease-Activated Receptor-1. *J Biol Chem* **283**:20600-20611.

McLaughlin JN, Shen L, Holinstat M, Brooks J D, Dibenedetto E and Hamm H E (2005) Functional Selectivity of G Protein Signaling by Agonist Peptides and Thrombin for the Protease-Activated Receptor-1. *J Biol Chem* **280**:25048-25059.

Means CK, Miyamoto S, Chun J and Brown J H (2008) S1P1 Receptor Localization Confers Selectivity for Gi-Mediated CAMP and Contractile Responses. *J Biol Chem* **283**:11954-11963.

Nicole O, Goldshmidt A, Hamill C E, Sorensen S D, Sastre A, Lyuboslavsky P, Hepler J R, McKeon R J and Traynelis S F (2005) Activation of Protease-Activated Receptor-1 Triggers Astrogliosis After Brain Injury. *J Neurosci* **25**:4319-4329.

Nishino A, Suzuki M, Ohtani H, Motohashi O, Umezawa K, Nagura H and Yoshimoto T (1993) Thrombin May Contribute to the Pathophysiology of Central Nervous System Injury. *J Neurotrauma* **10**:167-179.

Nurnberg A, Brauer A U, Wettschureck N and Offermanns S (2008) Antagonistic Regulation of Neurite Morphology Through Gq/G11 and G12/G13. *J Biol Chem* **19;283**:35526-35531.

Nystedt S, Emilsson K, Wahlestedt C and Sundelin J (1994) Molecular Cloning of a Potential Proteinase Activated Receptor. *Proc Natl Acad Sci U S A* **91**:9208-9212.

Offermanns S, Laugwitz K L, Spicher K and Schultz G (1994) G Proteins of the G12 Family Are Activated Via Thromboxane A2 and Thrombin Receptors in Human Platelets. *Proc Natl Acad Sci U S A* **91**:504-508.

Ogino Y, Tanaka K and Shimizu N (1996) Direct Evidence for Two Distinct G Proteins Coupling With Thrombin Receptors in Human Neuroblastoma SH-EP Cells. *Eur J Pharmacol* **316**:105-109.

Olianas MC, Dedoni S and Onali P (2007) Proteinase-Activated Receptors 1 and 2 in Rat Olfactory System: Layer-Specific Regulation of Multiple Signaling Pathways in the Main Olfactory Bulb and Induction of Neurite Retraction in Olfactory Sensory Neurons. *Neuroscience* **146**:1289-1301.

Oron Y, Dascal N, Nadler E and Lupu M (1985) Inositol 1,4,5-Trisphosphate Mimics Muscarinic Response in Xenopus Oocytes. *Nature* **313**:141-143.

Ossovskaya VS and Bunnett N W (2004) Protease-Activated Receptors: Contribution to Physiology and Disease. *Physiol Rev* **84**:579-621.

Pindon A, Berry M and Hantai D (2000) Thrombomodulin As a New Marker of Lesion-Induced Astrogliosis: Involvement of Thrombin Through the G-Protein-Coupled Protease-Activated Receptor-1. *J Neurosci* **20**:2543-2550.

Post GR, Collins L R, Kennedy E D, Moskowitz S A, Aragay A M, Goldstein D and Brown J H (1996) Coupling of the Thrombin Receptor to G12 May Account for Selective Effects of Thrombin on Gene Expression and DNA Synthesis in 1321N1 Astrocytoma Cells. *Mol Biol Cell* **7**:1679-1690.

Ramachandran R, Mihara K, Mathur M, Rochdi M D, Bouvier M, Defea K and Hollenberg M D (2009) Agonist-Biased Signaling Via Proteinase Activated Receptor-2: Differential Activation of Calcium and MAPkinase Pathways. *Mol Pharmacol*.

Sorensen SD, Nicole O, Peavy R D, Montoya L M, Lee C J, Murphy T J, Traynelis S F and Hepler J R (2003) Common Signaling Pathways Link Activation of Murine PAR-1, LPA, and S1P Receptors to Proliferation of Astrocytes. *Mol Pharmacol* **64**:1199-1209.

Swift S, Leger A J, Talavera J, Zhang L, Bohm A and Kuliopulos A (2006) Role of the PAR1 Receptor 8th Helix in Signaling: the 7-8-1 Receptor Activation Mechanism. *J Biol Chem* **281**:4109-4116.

Traynelis SF and Trejo J (2007) Protease-Activated Receptor Signaling: New Roles and Regulatory Mechanisms. *Curr Opin Hematol* **14**:230-235.

Vandell AG, Larson N, Laxmikanthan G, Panos M, Blaber S I, Blaber M and Scarisbrick I A (2008) Protease-Activated Receptor Dependent and Independent Signaling by Kallikreins 1 and 6 in CNS Neuron and Astroglial Cell Lines. *J Neurochem* **107**:855-870.

Vanhauwe JF, Thomas T O, Minshall R D, Tiruppathi C, Li A, Gilchrist A, Yoon E J, Malik A B and Hamm H E (2002) Thrombin Receptors Activate G(o) Proteins in Endothelial Cells to Regulate Intracellular Calcium and Cell Shape Changes. *J Biol Chem* **277**:34143-34149.

Verrall S, Ishii M, Chen M, Wang L, Tram T and Coughlin S R (1997) The Thrombin Receptor Second Cytoplasmic Loop Confers Coupling to Gq-Like G Proteins in Chimeric Receptors. Additional Evidence for a Common Transmembrane Signaling and G Protein Coupling Mechanism in G Protein-Coupled Receptors. *J Biol Chem* **272**:6898-6902.

Voss B, McLaughlin J N, Holinstat M, Zent R and Hamm H E (2007) PAR1, but Not PAR4, Activates Human Platelets Through a Gi/o/Phosphoinositide-3 Kinase Signaling Axis. *Mol Pharmacol* **71**:1399-1406.

Vu TK, Hung D T, Wheaton V I and Coughlin S R (1991) Molecular Cloning of a Functional Thrombin Receptor Reveals a Novel Proteolytic Mechanism of Receptor Activation. *Cell* **64**:1057-1068.

Wang H, Ubl J J, Stricker R and Reiser G (2002) Thrombin (PAR-1)-Induced Proliferation in Astrocytes Via MAPK Involves Multiple Signaling Pathways. *Am J Physiol Cell Physiol* **283**:C1351-C1364.

Xu WF, Andersen H, Whitmore T E, Presnell S R, Yee D P, Ching A, Gilbert T, Davie E W and Foster D C (1998) Cloning and Characterization of Human Protease-Activated Receptor 4. *Proc Natl Acad Sci U S A* **95**:6642-6646.

Molecular Pharmacology Fast Forward. Published on March 9, 2010 as DOI: 10.1124/mol.109.062018
This article has not been copyedited and formatted. The final version may differ from this version.

Footnotes

This work was supported by National Institutes of Health grants [R01NS049195, R01NS37112, R01NS039419] and by an American Heart Association grant [0715465B].

Reprint requests should go to:

John R. Hepler, Ph.D.

Emory University School of Medicine

Department of Pharmacology

1510 Clifton Road

Atlanta GA 30322

jhepler@emory.edu

Molecular Pharmacology Fast Forward. Published on March 9, 2010 as DOI: 10.1124/mol.109.062018
This article has not been copyedited and formatted. The final version may differ from this version.

Legends for Figures

Figure 1. PAR1 and PAR2 activate multiple G protein-regulated signaling responses. A) [^{3}H]Inositol phosphate accumulation in intact COS-7 cells were transfected with the indicated PAR cDNA as described under "Materials and Methods." After a 5 h transfection period, cells were metabolically labeled overnight with 4 µCi/mL *myo*-[^{3}H]inositol in serum-free media. Following a 20 min incubation at 37°C in 10 mM $LiCl_2$, cells were either left unstimulated or were activated with 30µM TFLLR or 10µM LIGRLO. To stop the reaction, cells were solubilized with 20 mM formic acid, and lysates were neutralized with 0.7 M NH_4OH. [^{3}H]InsPs fractions were separated by anion exchange chromatography, and total [^{3}H]InsP content was assessed by liquid scintillation spectrometry. Data are presented as the average of total InsPs from 3 different experiments (mean cpm + S.E.M; each point performed in triplicate). B) 5 ng of PAR1 or PAR2 cRNA was injected into *X. laevis* oocytes, which were maintained in 1x Barth's solution. 4-5 days after injection, oocyte $I_{Ca(Cl)}$ measurements were obtained in response to stimulation by either 30µM TFLLR or 10µM LIGRLO using a two-electrode voltage clamp, as described. Data is expressed as the mean change in $I_{Ca(Cl)}$ + S.E.M. (n>11 oocytes). C) Vector alone, PAR1 or PAR2 were separately transfected into COS-7 cells. Cells were either unstimulated or stimulated with, 30µM TFLLR or 10µM LIGRLO, as indicated, for 2 min. Immunoblots were performed with either phospho-ERK1/2 or total ERK1/2 antibodies followed by a goat-anti rabbit secondary antibody or with an HRP-conjugated anti-HA antibody and detected by ECL. D) PAR-mediated RhoA activation was measured using a RhoA G-LISA™ Assay kit. First, PAR cDNA was separately transfected into COS-7 cells for 5 h before the media was replaced with serum-free media overnight. The following day, cells were either left unstimulated or were activated with 30µM TFLLR or 10µM LIGRLO for 2 min before cell lysis. After following the manufacturer's protocol, the absorbance of each well was read with a spectrophotometer wavelength of 490nm.

Molecular Pharmacology Fast Forward. Published on March 9, 2010 as DOI: 10.1124/mol.109.062018
This article has not been copyedited and formatted. The final version may differ from this version.

Figure 2. PAR1 and PAR2 form stable complexes with distinct sets of G proteins. Twenty-four hours after co-transfection with separate receptor/G protein pairs and controls (as indicated), cells were lysed, harvested, and sonicated in Tris Buffer. Proteins were extracted from membranes with 2% DβM (3 h, 4°C) and IP'ed overnight at 4°C with anti-FLAG affinity gel. Immunoprecipitates were resolved by SDS-PAGE (11% polyacrylamide). Proteins were immunoblotted and visualized with ECL. *Top panel,* Western blot analysis of IP'ed G proteins with corresponding G protein-specific antibodies. *Bottom panel,* Western blot analysis of cell lysates (input) with corresponding G protein-specific antibodies. Results are representative of at least three separate experiments.

Figure 3. PAR1 and PAR2 form stable complexes with G protein heterotrimers. Co-IP studies were performed as described but for these experiments; either $G\alpha_o$or $G\alpha_{11}$ was co-transfected with PAR1 or PAR2 and pulled down in the presence of GTPγS, in the presence and absence of agonist. Here, we have also used a pan-Gβ antibody to detect the presence of endogenous Gβ in the receptor/Gα complex. *Top panel,* Western blot analysis of IP'ed G proteins with corresponding G protein-specific antibodies. *Bottom panel,* Western blot analysis of cell lysates (input) with corresponding G protein-specific antibodies. Antibodies to $G\alpha_o$ and to $G\alpha_{11}$ were mixed in one tube to blot the entire membrane at once. The same goat anti-rabbit secondary antibody was then used, and proteins were visualized using ECL.

Figure 4. PAR1, but not PAR2, inhibits the accumulation of cAMP and stimulates ERK1/2 phosphorylation in a PTX-sensitive manner. The inhibition of cAMP accumulation and stimulated ERK1/2 phosphorylation were measured in COS-7 cells over-expressing PAR1 or PAR2. A,B) All PAR-expressing COS-7 cells were stimulated with 10μM isoproterenol in the presence of 100μM IBMX. Some cells also were activated with 30μM TFLLR or 10μM LIGRLO

Molecular Pharmacology Fast Forward. Published on March 9, 2010 as DOI: 10.1124/mol.109.062018
This article has not been copyedited and formatted. The final version may differ from this version.

for 2 min in the presence and absence of 100 ng/mL PTX. Lysates were added to a 96-well ELISA plate, provided in the cAMP assay kit (Cell Biolabs). After following the manufacturer's protocol, cAMP levels were measured using a spectrophotometer. Results are expressed as the average + S.E.M. of 3 different experiments. C,D) COS-7 cells expressing PAR1 or PAR2 were serum-starved overnight and stimulated with 30μM TFLLR or 10μM LIGRLO for 2 min in the presence and absence of 100 ng/mL PTX. Cells were lysed and harvested in 2X Laemelli buffer, sonicated and subjected to SDS-PAGE. Western blots were performed with phospho-ERK1/2 and total ERK1/2 antibodies. Protein bands were detected by ECL.

Figure 5. PAR1 and PAR2 both utilize $G_{q/11}$ to activate PLC-β signaling and $G_{12/13}$ to activate Rho. A) PAR-mediated RhoA activation was measured using a RhoA G-LISA™ Assay kit as described in Figure 1. PARs were transfected either alone or in combination with p115-RGS cDNA into COS-7 cells, serum-starved overnight, and stimulated with 30μM TFLLR or 10μM LIGRLO for 2 min before cell lysis. Lysates were added to the ELISA plate supplied in the G-LISA™ Assay kit and the manufacturer's protocol was followed. The absorbance of each well was read with a spectrophotometer wavelength of 490nm. Data are presented as the average RhoA activation from three different experiments (fold over basal + S.E.M.; each point performed in duplicate). B) As described for Figure 1, [^{3}H]InsP accumulation in intact COS-7 cells were transfected with the indicated PAR alone or in the presence of the specific G protein inhibitor (GRK2-RGS or p115-RGS), pre-labeled with 4 μCi/ml *myo*-[^{3}H]inositol, incubated with $LiCl_2$, and activated with 30μM TFLLR or 10μM LIGRLO for 30 min. After solubilization, lysates were neutralized and separated by anion exchange chromatography. Data are presented as the average of total InsPs from three different experiments (% maximal InsPs + S.E.M; each point performed in triplicate).

Molecular Pharmacology Fast Forward. Published on March 9, 2010 as DOI: 10.1124/mol.109.062018
This article has not been copyedited and formatted. The final version may differ from this version.

Figure 6. PAR1 and PAR2 both utilize $G_{q/11}$-linked pathways to activate inositol phosphate signaling and $G_{12/13}$-linked pathways to activate RhoA. A) [^{3}H]InsP accumulation was measured in Neu7 cells in the presence and absence of pharmacological inhibitors of PLC (10μM U73122; added 30 min prior to stimulation) or Rho (1 μg/mL C3 toxin; added 4 h prior to stimulation) signaling. Cells were stimulated with 100μM TFLLR or 10μM LIGRLO for 30 min before solubilization. Then lysates were neutralized and separated by anion exchange chromatography. Data are presented from three different experiments (fold over basal InsPs + S.E.M; each point performed in triplicate). B) Similar to Figs. 1 and 5, PAR-mediated RhoA activation in Neu7 cells was measured using a RhoA G-LISA™ Assay kit. Cells were serum-starved overnight, and during the final 4 hours of stimulation, 1 μg/mL C3 toxin was added to appropriate wells. Cells were then stimulated with 100μM TFLLR or 200μM LIGRLO for 2 min before cell lysis. Lysates were placed in the G-LISA™ plate and the manufacturer's protocol was followed. The absorbance of each well was read with a spectrophotometer wavelength of 490nm. Data are presented as the average RhoA activation from three different experiments (fold over basal + S.E.M.; each point performed in duplicate).

Figure 7. PARs stimulate ERK1/2 phosphorylation in Neu7 cells. A-B) Neu7 cells were serum-starved overnight in the presence of a range of PTX concentrations (0-300 ng/mL), and stimulated with either nothing, 100μM TFLLR or 200μM LIGRLO, as indicated. Densitometry was performed on three independent experiments and phospho-ERK1/2 levels were normalized to total ERK levels. C) Neu7 cells were serum-starved overnight. Prior to stimulation with either 100μM TFLLR or 200μM LIGRLO, inhibitors to PKC (1μM BIS; 30 min) PLC (10μM U73122; 30 min), or Rho (1 μg/mL C3 toxin, 4 h) were added to the serum-free media. Densitometry was performed on three independent experiments and phospho-ERK1/2 levels were normalized to total ERK levels. All immunoblots were performed with either phospho-ERK1/2 or total ERK1/2 antibodies and protein bands were detected by ECL.

Molecular Pharmacology Fast Forward. Published on March 9, 2010 as DOI: 10.1124/mol.109.062018
This article has not been copyedited and formatted. The final version may differ from this version.

Figure 8. PAR1 and PAR2, stimulation of Neu7 cell migration involves ERK-mediated pathways but only PAR1-induced migration is PTX-sensitive A) Neu7 cells were "wounded" with a 10µL pipette tip that was dragged across each monolayer of a 6-well plate. Cells were then serum-starved in the presence and absence of 100 ng/mL PTX or 10µM U0126 and then treated with either vehicle, 100µM TFLLR, or 200µM LIGRLO for an additional 24 h. Pictures were taken with an Olympus IX51 light microscope after 0 h and 24 h of agonist addition. Images shown are representative of three different experiments. B) Cell migration into the wounded area from the images in (A) and also from a different set of similar images was quantified using ImageJ software. For each condition pairings, the cell-free areas were subtracted from the total area of the wound to obtain the area covered by cells. This number was then divided by the total area value to obtain a percent value. C. Confluent Neu7 cells were serum-starved for 24 h prior to treatment with either vehicle, 100uM TFLLR, or 200uM LIGRLO for an additional 24 h. [^{3}H]thymidine was added to the cells for the final 2 h of the experiment and was recovered in the acid-insoluble material at the end of the experiment. Data are reported as the average of four different experiments (% max TFLLR stimulation + S.E.M.).

Figure 1

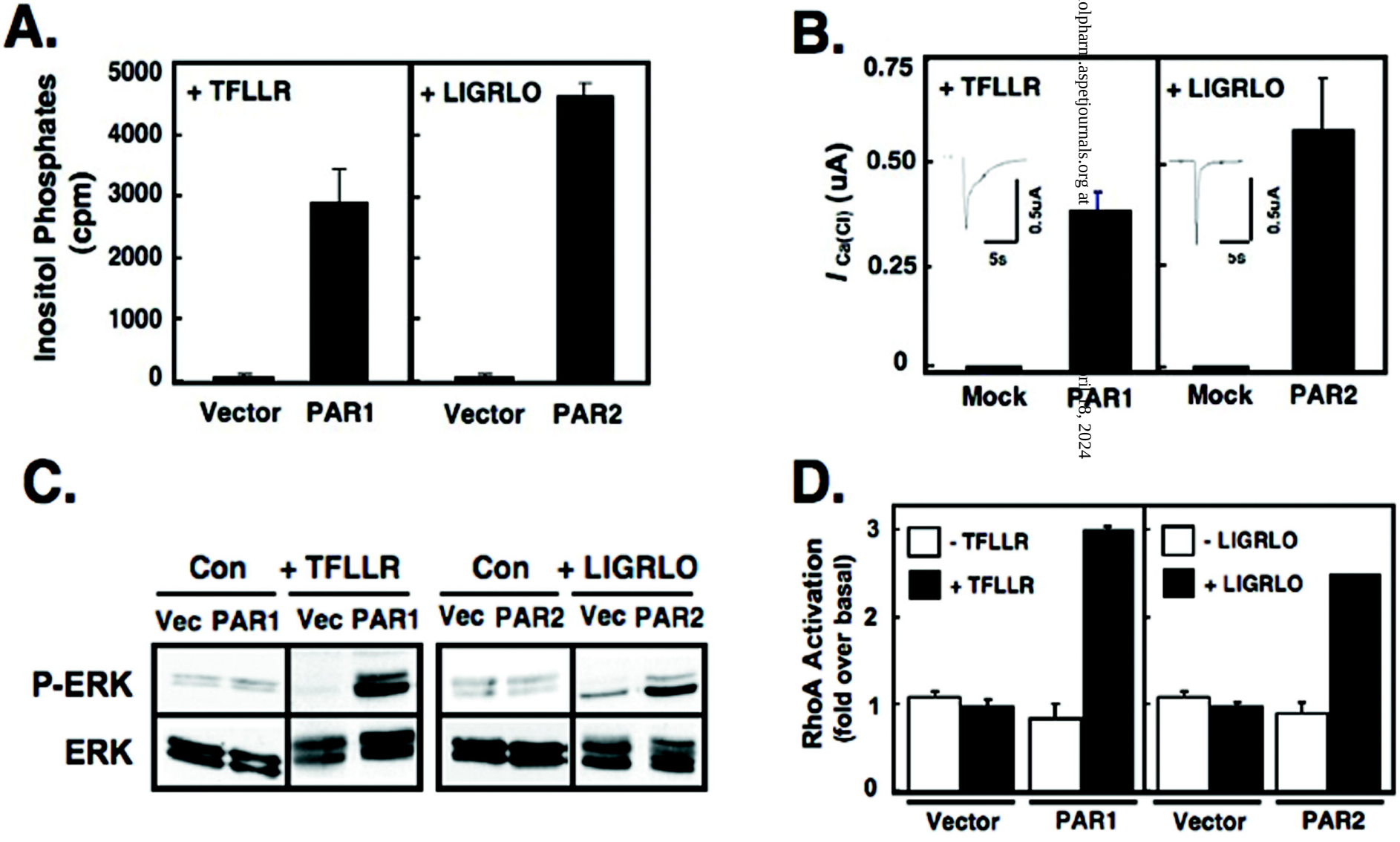

Figure 2

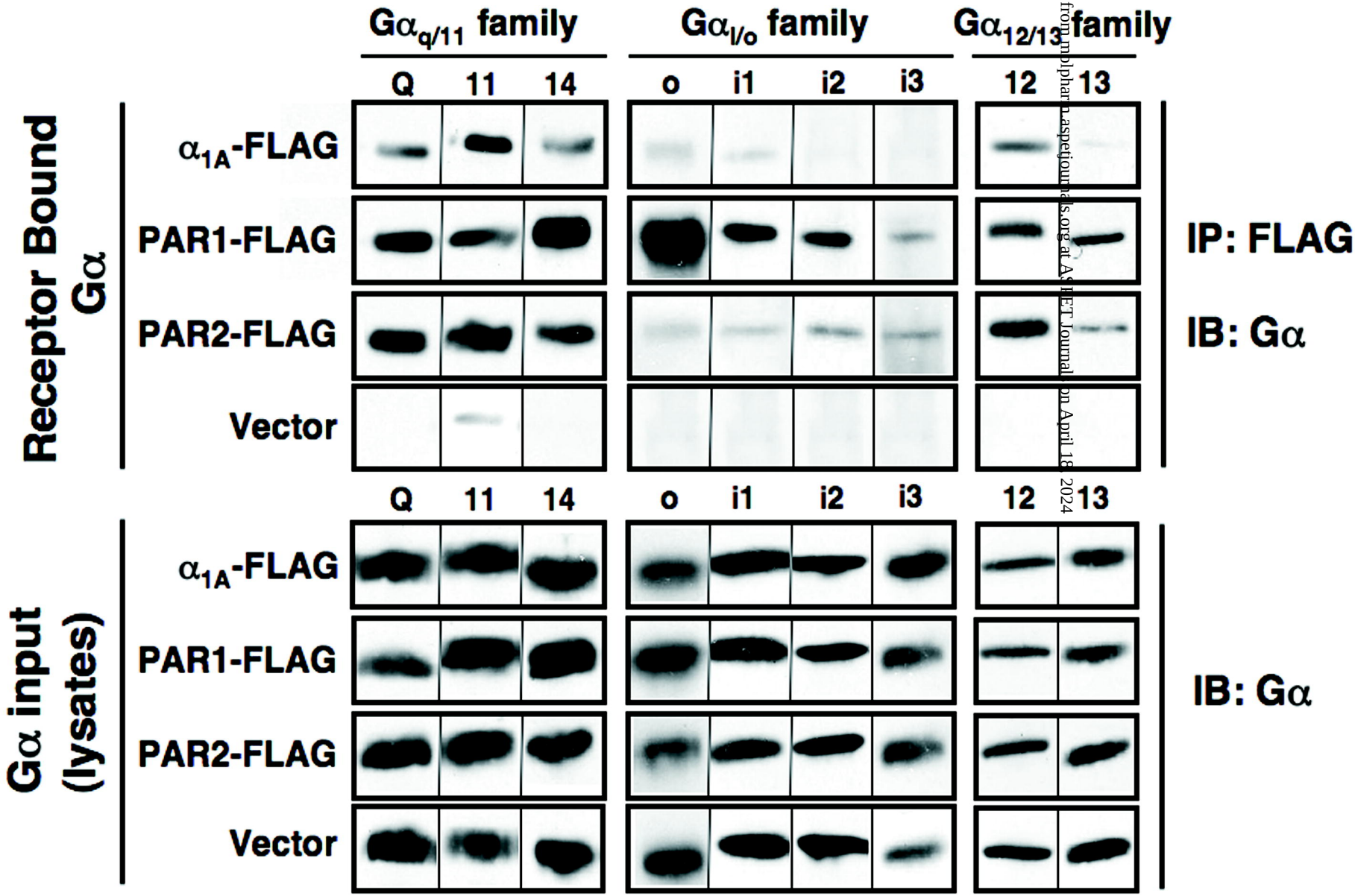

Figure 3

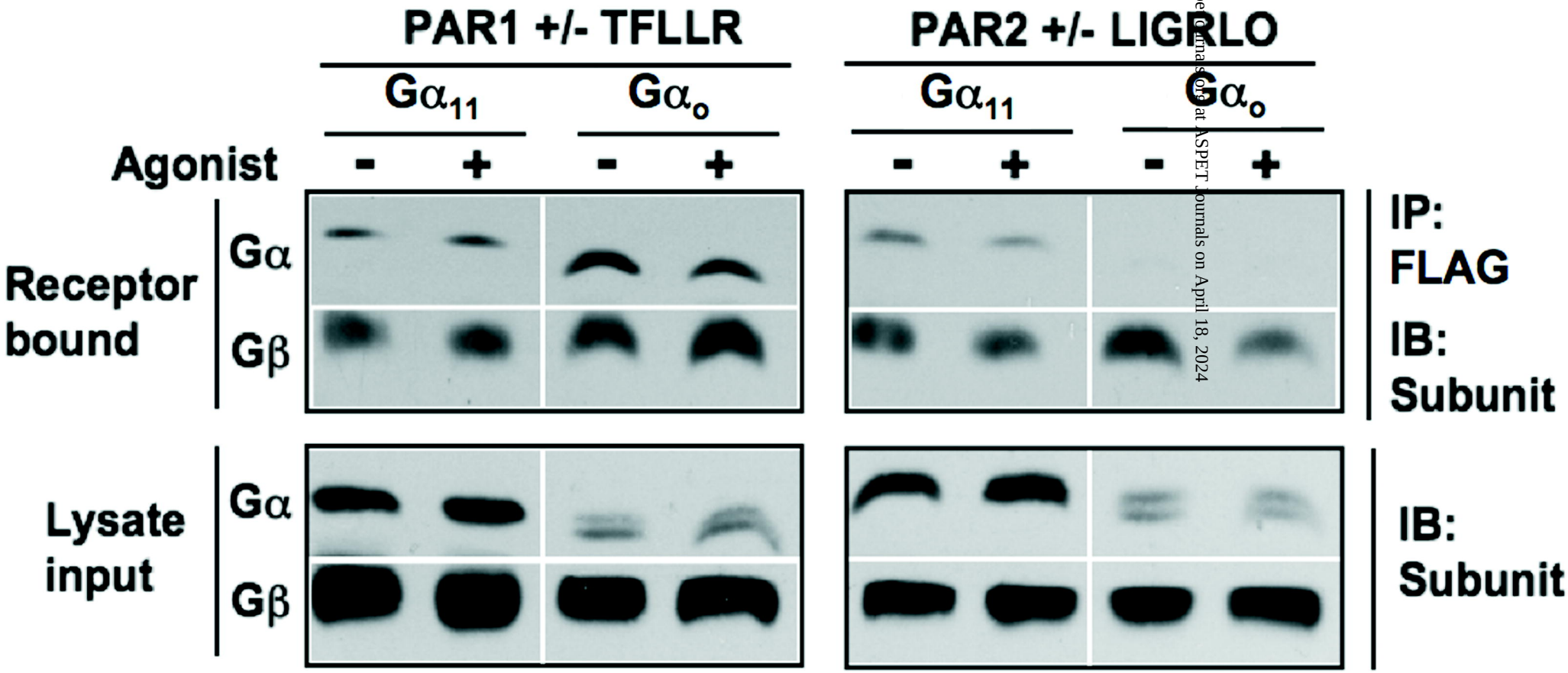

Figure 4

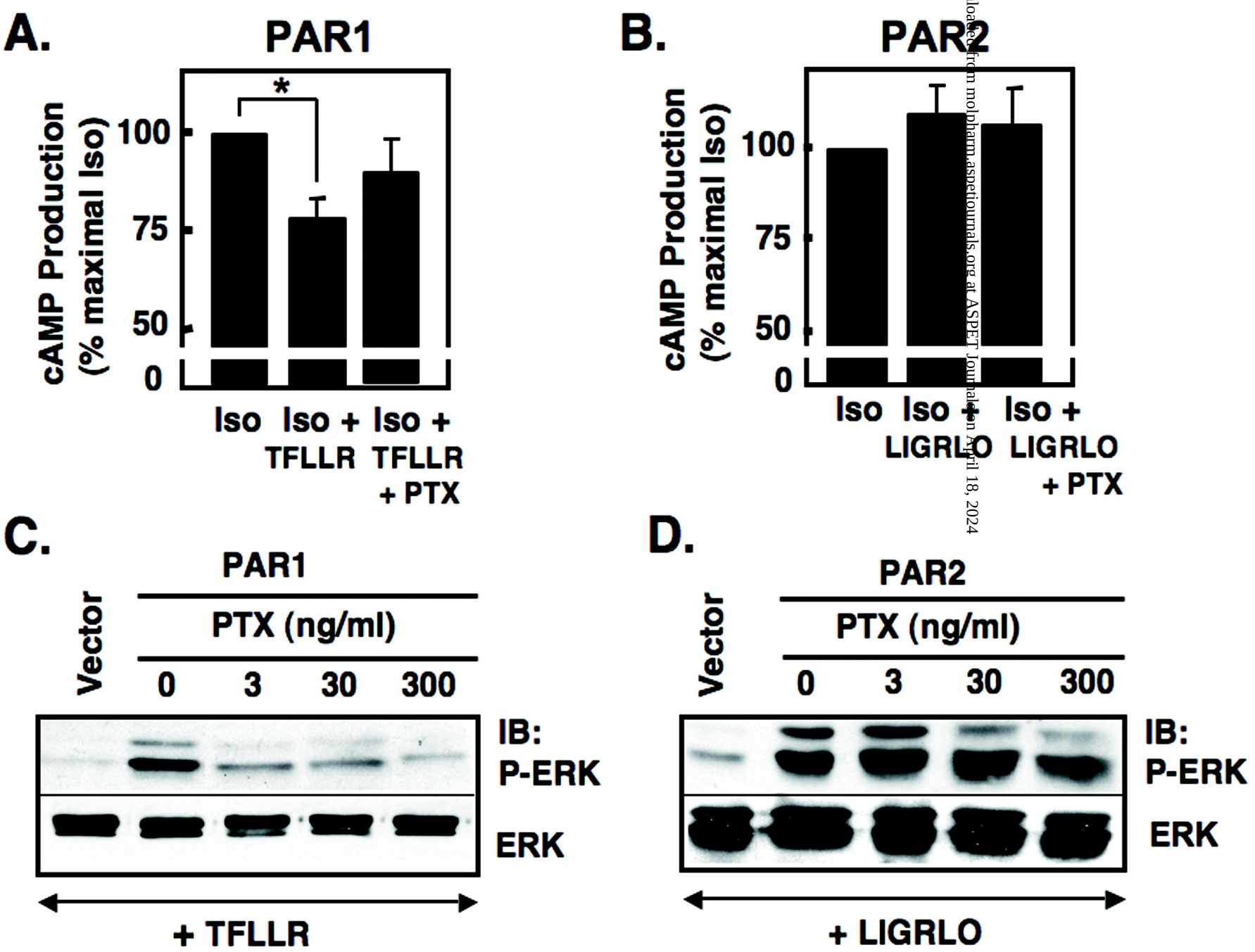

Figure 5

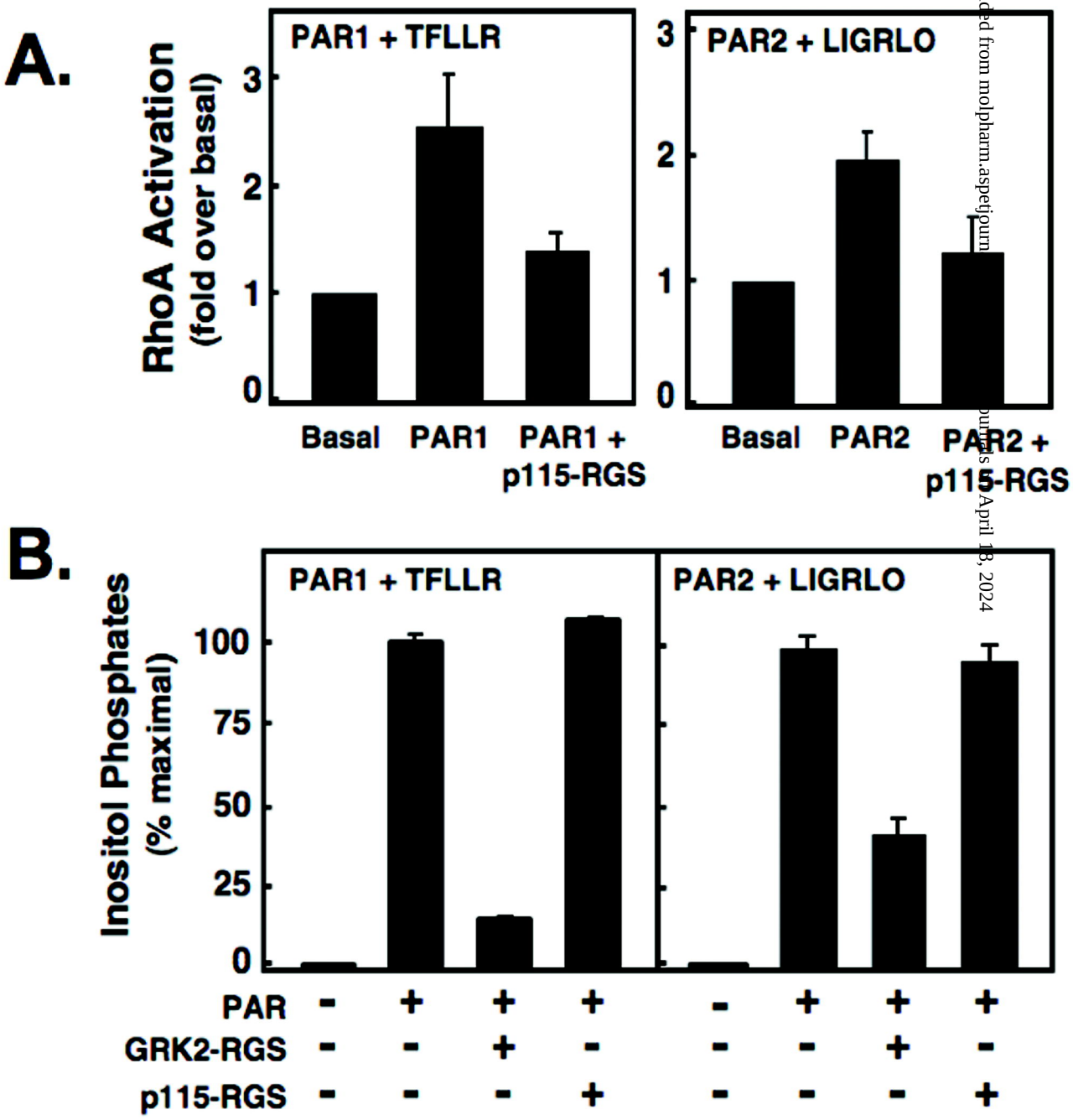

Figure 6

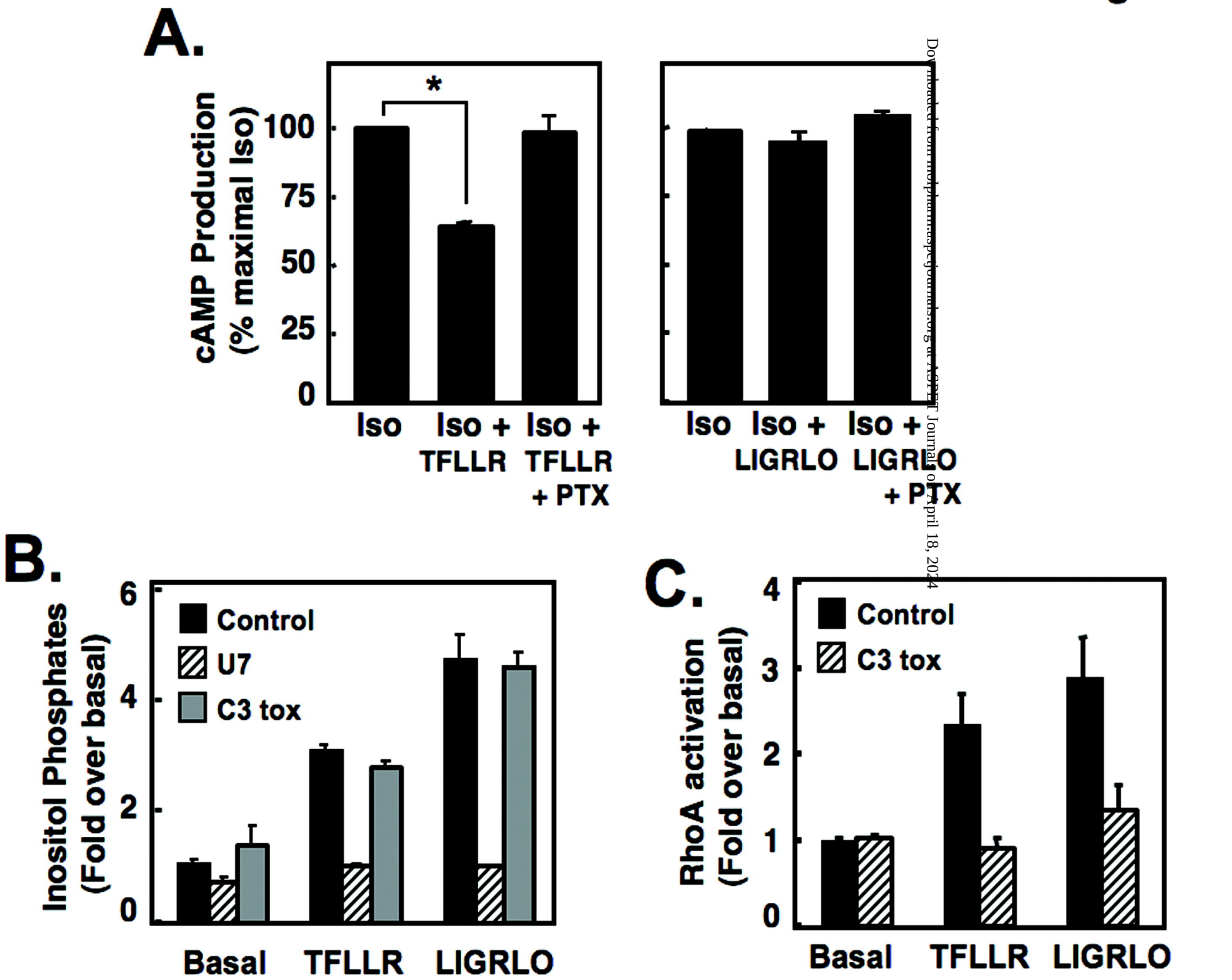

Figure 7

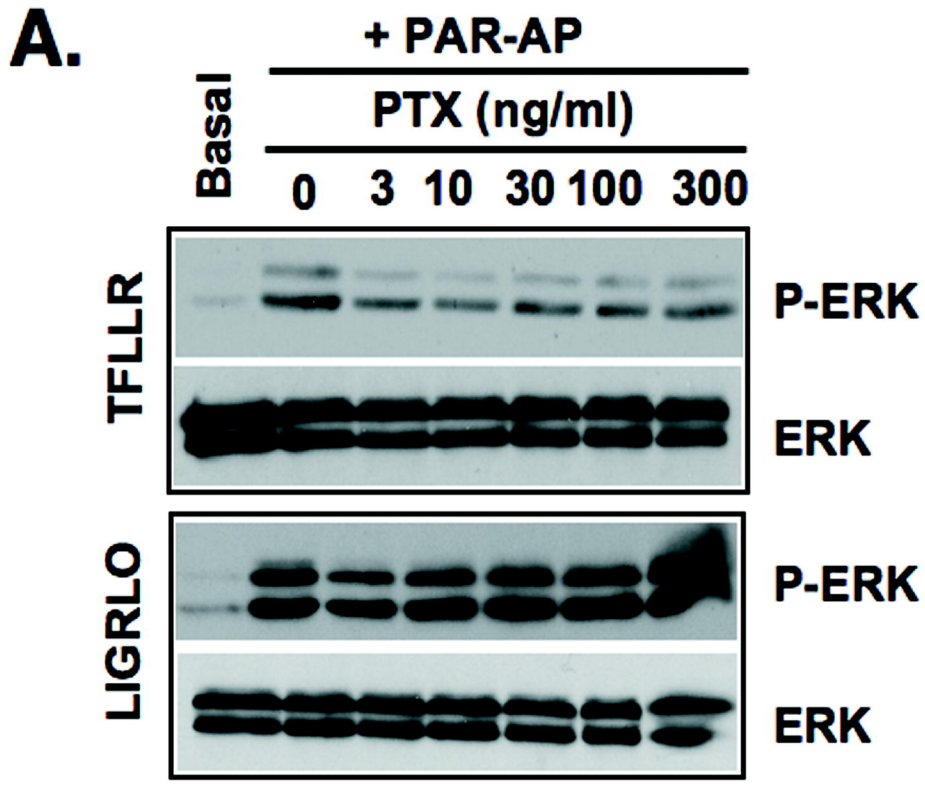

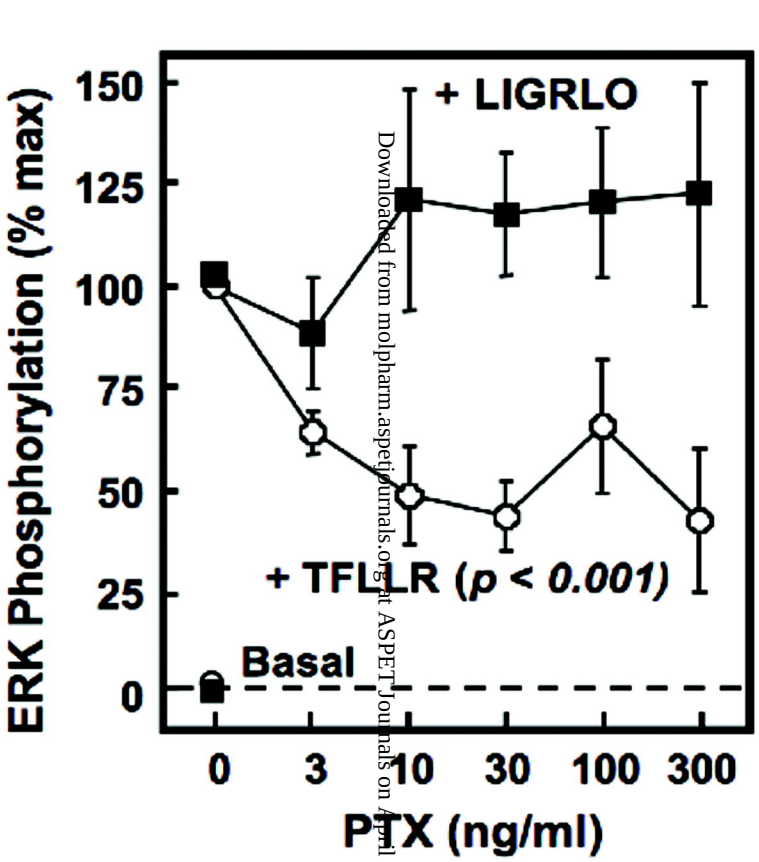

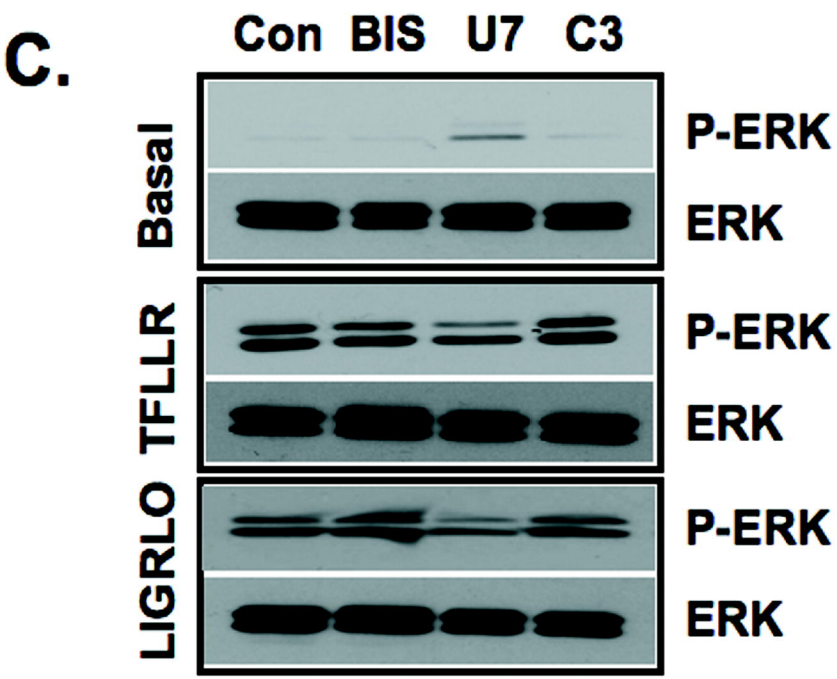

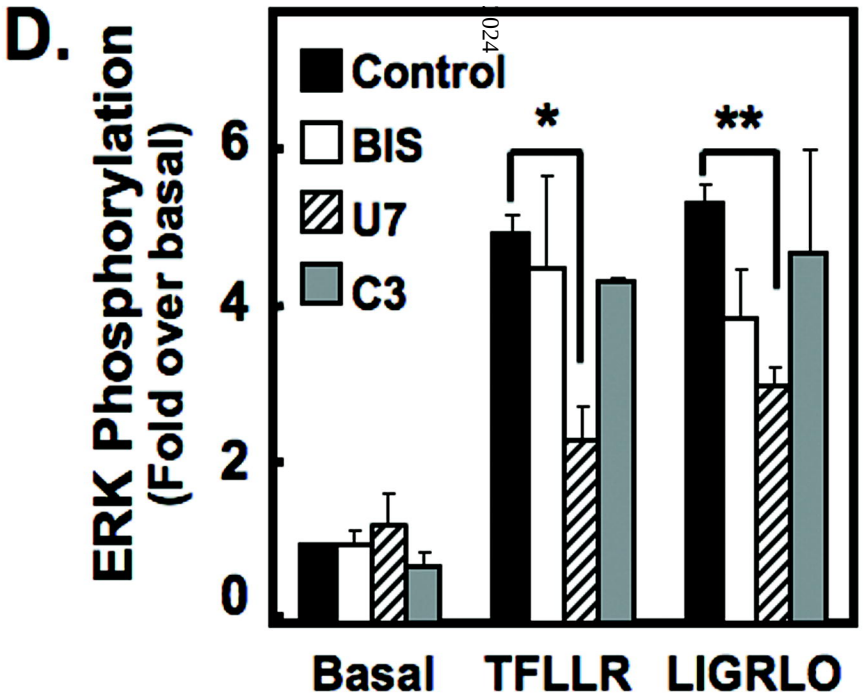

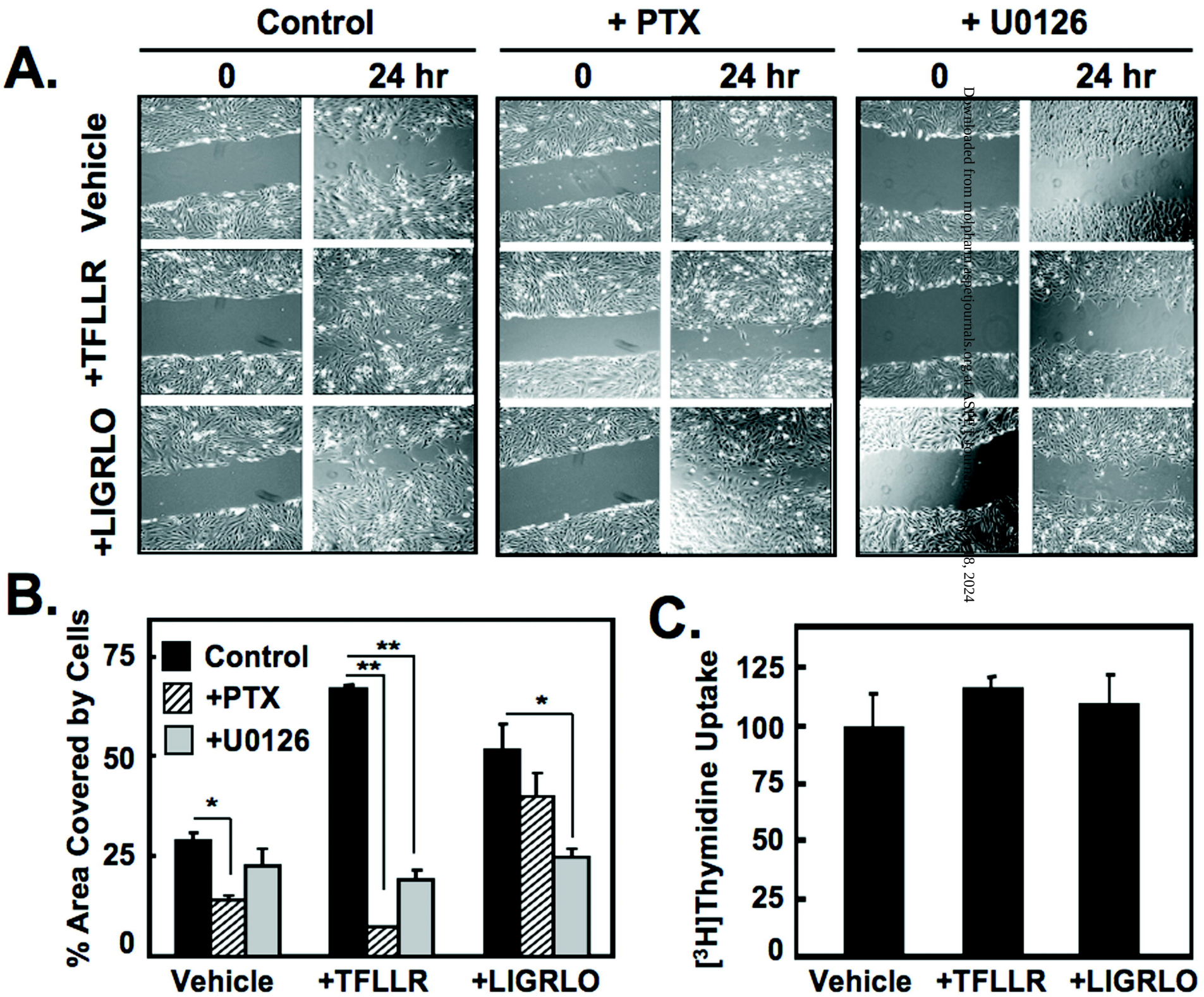

Figure 8